

All previously published papers were reproduced with permission from the publisher

Published and printed by Karolinska University Press
Box 200, SE-171 77 Stockholm, Sweden

© Magnus Schou, 2006
ISBN 91-7140-773-1

ABSTRACT

The noradrenergic (NE), serotonergic (5-HT) and dopaminergic (DA) neurotransmission systems all have specific proteins responsible for the regulation of synaptic concentrations of neurotransmitter in the central nervous system (CNS) and in the periphery. Several reports have shown that the expression of these proteins, the monoamine transporters, within the CNS, may be altered in patients with certain neurodegenerative or neuropsychiatric disorders. Positron emission tomography (PET) is an imaging technique that enables quantitative studies in high resolution of receptor or transporter proteins inside the living human brain. At the outset of research for this thesis, PET had been used successfully in the mapping of 5-HT and DA transporters, but not NE transporters (NETs). The aim of this thesis was to develop a radioligand suitable for imaging NETs in the human brain *in vivo*.

This project focused on the screening of candidate NET radioligands by emission measurements in cynomolgus monkeys *in vivo*. Concomitant with these studies, radiometabolite analyses were performed on peripheral monkey plasma. To further characterise radioligands, *in vitro* autoradiography studies were performed on *post mortem* human brain tissue. During this screening process, nine of the most potent and selective NET inhibitors reported to date were prepared and labeled with carbon-11 ($t_{1/2}$ 20.4 min) or fluorine-18 ($t_{1/2}$ 109.8 min). Some improvements were also made with regards to the labelling of aryl fluoromethyl ethers and sulfides with fluorine-18, with a view to potential application in preparing new candidate NET radioligands.

Several candidate radioligands failed in the initial screening process. However, one lead compound was identified, namely (S,S)-[^{11}C]MeNER. The regional distribution of (S,S)-[^{11}C]MeNER in monkey brain was found to be in accord with known densities of NETs and was also shown to be specific to NET in a pre-treatment experiment. However, the binding kinetics of (S,S)-[^{11}C]MeNER was found to be slow, which limited its utility in assessing regional NET densities in man. (S,S)-[^{18}F]FMeNER was therefore developed as an improved analogue with a longer half-life that allowed the specific binding to reach equilibrium during the time-frame of the PET measurements. Its metabolic instability did however result in defluorination, which confounded the imaging of cortical regions. The di-deuterated analogue (S,S)-[^{18}F]FMeNER-D₂ was thus prepared, which showed a similar distribution in brain as the previously mentioned radioligands, but also displayed a reduced defluorination. *In vitro* autoradiography with (S,S)-[^{18}F]FMeNER-D₂ on *post mortem* human brain cryosections further demonstrated specific binding to NET. (S,S)-[^{18}F]FMeNER-D₂ has the potential to be the first useful radioligand for quantitative imaging of NETs in the living human brain.

KEY WORDS: PET, Radioligand, NET, Brain

Logic will get you from A to B. Imagination will take you everywhere.

Albert Einstein

Till Sara

LIST OF PUBLICATIONS

This thesis is based on the following papers and manuscripts (I-VII):

- I. Schou M., Sóvágó J., Pike VW., Gulyás B., Bøgesø KP., Farde L., Halldin C. Synthesis and positron emission tomography evaluation of three norepinephrine transporter radioligands. [^{11}C]desipramine, [^{11}C]talopram and [^{11}C]talsupram. *Mol Imaging Biol* 2006;8:1-8.
- II. Schou M., Halldin C., Sóvágó J., Pike VW., Gulyás B., Mozley PD., Johnson DP., Hall H., Innis RB., Farde L. Specific in vivo binding to the norepinephrine transporter demonstrated with the PET radioligand, (S,S)-[^{11}C]MeNER. *Nucl Med Biol* 2003;30:707-14.
- III. Schou M., Halldin C., Sóvágó J., Pike VW., Hall H., Gulyás B., Mozley PD., Dobson D., Shchukin E., Innis RB., Farde L. PET evaluation of novel radiofluorinated reboxetine analogs as norepinephrine transporter probes in the monkey brain. *Synapse* 2004;53:57-67
- IV. Schou M., Halldin C., Pike VW., Mozley PD., Dobson D., Innis RB., Farde L., Hall H. Post-mortem human brain autoradiography of the norepinephrine transporter using (S,S)-[^{18}F]FMeNER-D₂. *Eur Neuropsychopharmacol* 2005;15:517-20.
- V. Schou M., Pike VW., Sóvágó J., Gulyás B., Gallagher PT, Dobson D., Walter MW., Rudyk H., Farde L., Halldin C. Synthesis of ^{11}C -labelled hydroxylated analogs of (S,S)-MeNER and DMI and their evaluation as candidate radioligands for imaging norepinephrine transporters with PET. *Manuscript*
- VI. Schou M., Pike VW., Varrone A., Gulyás B., Farde L., Halldin C. Synthesis and PET evaluation of (R)-[S-methyl- ^{11}C]thionisoxetine, a candidate radioligand for imaging brain norepinephrine transporters. *Manuscript*
- VII. Schou M., Zoghbi SS., Shetty HU., Shchukin E., Liow J-S., Hong J., Andrée BA., Gulyás B., Farde L., Innis RB., Pike VW., Halldin C. Investigation of the metabolites of (S,S)-[^{11}C]MeNER in humans, monkeys and rats. *Manuscript*

CONTENTS

ABSTRACT	3
LIST OF PUBLICATIONS	5
CONTENTS	6
LIST OF ABBREVIATIONS	7
INTRODUCTION	9
AIMS AND LONG TERM OBJECTIVES	17
RESULTS & DISCUSSION	17
Bicyclic and Tricyclic NET inhibitors as PET radioligands (Paper I)	17
Candidate Radioligands Based on Aryloxy Morpholines (Papers II-V)	19
Analysis of Metabolites of (S,S)-[¹¹ C]MeNER in Rats, Monkeys and Humans (Paper VII)	21
Fluorinated Analogues of (S,S)-MeNER (Paper III)	23
In vitro Imaging of NET using (S,S)-[¹⁸ F]FMeNER-D ₂ (Paper IV)	25
One-Pot Syntheses of [¹⁸ F]Fluoromethyl Ethers and Sulfides (Unpublished Results)	26
Hydroxylated Analogues of DMI and (S,S)-MeNER (Paper V)	29
(R)-[¹¹ C]Thionisoxetine – a High Affinity NET Radioligand (Paper VI)	31
CONCLUSIONS	36
REFERENCES	37
ACKNOWLEDGMENTS	47

LIST OF ABBREVIATIONS

5-HT	serotonin
a.k.a	also known as
ADHD	attention deficit hyperactivity disorder
Alpha particle	positive helium ion (He^{2+})
BBB	blood-brain barrier
Bn	benzyl
Carrier	non-radioactive form of a radioligand/radiotracer (e.g. with $^{12/13}\text{C}$ replacing ^{11}C)
CNS	central nervous system
DA	dopamine
DAT	dopamine transporter
DMF	<i>N,N</i> -dimethylformamide
DMI	desipramine, desmethyl-imipramine
Et	ethyl
Eudismic ratio	potency of the active enantiomer relative to that of the inactive enantiomer
Eutomer	active enantiomer
HPLC	high performance liquid chromatography
Hydrophilic	polar, tendency to dissolve well in water
I.D.	injected dose
<i>In vitro</i>	“in flask”, i.e. in the test tube
<i>In vivo</i>	“in life”, i.e. in the living cell or organism
Kryptofix (K2.2.2)	4,7,13,16,21,24-Hexaoxa-1,10-diazabicyclo [8.8.8]hexacosane
LC	locus coeruleus
Lipophilic	non-polar, tendency to not dissolve well in water
Me	methyl
MeCN	acetonitrile
MeNER	methyl norethyl reboxetine
Ms	methanesulfonyl
NE	norepinephrine
NET	norepinephrine transporter
Norepinephrine	noradrenaline

P	partition coefficient between octanol/water, used as an index of hydrophilicity/lipophilicity
PET	positron emission tomography
Ph	phenyl
Pr	propyl
PVE	partial volume effect
RCY	radiochemical yield
RN	raphe nuclei
ROI	region of interest
SAR	structure activity relationships
SERT	serotonin transporter
SPET	single photon emission tomography
SR	specific radioactivity
SSRI	selective serotonin reuptake inhibitor
$t_{1/2}$	half-life
Tf	triflate, trifluoromethanesulfonyl
TFA	trifluoroacetic acid
TLC	thin layer chromatography
Ts	tosyl, <i>p</i> -toluenesulfonyl
<i>Vide infra</i>	see below
<i>Vide supra</i>	see above

INTRODUCTION

Towards the end of the 19th century, the German scientist Paul Ehrlich was fascinated by how dyes could selectively stain certain cell types in the presence of others. Ehrlich knew that the colour of the dye was associated with the side-chains of its chemical structure and therefore assumed that cells had similar side-chains, which interacted with the side-chains of the dyes in a specific manner. This led him to believe that for each strain of bacteria, there was a specific compound, a so-called “magic bullet”, which could kill the bacteria without harming the host. In 1909, after extensive synthesis and biological testing, Ehrlich found an arsenic compound, “compound 606”, which turned out to be an effective cure for syphilis. Ehrlich is considered one of the pioneers in medicinal chemistry and his “compound 606”, later known as Salvarsan, was used until antibiotics were discovered in the 1940s.

The imaging agents used with positron emission tomography (PET) today can be viewed as the present “magic bullets”. Similar to Ehrlich’s original idea, suitable PET imaging agents seek out and image their respective targets with very high selectivity. This thesis work has focused on the development of new agents for imaging norepinephrine transporters inside the living human brain. The present summary will begin by briefly introducing the importance of norepinephrine transporters in human psychobiology and what knowledge that might be gained by developing suitable imaging agents for these transporter proteins. Some of the methodology that is employed in radioligand synthesis and development will also be described. The specific results that were obtained during this project will be summarized here, as well as in appendices as manuscripts or reprints from original publications. The thesis will be concluded with some views on future directions in the development of norepinephrine transporter radioligands.

Norepinephrine and Norepinephrine Transporters

Norepinephrine (NE, noradrenaline) is a chemical messenger that is part of a greater family of hormones and neurotransmitters commonly referred to as catecholamines. The catecholamines, especially NE and epinephrine (E, adrenaline), play a central role in the regulation of heart rate and glucose metabolism and are vital in preparing the body for fight or flight responses.¹ Within the central nervous system (CNS), NE acts as a neurotransmitter that is involved in a number of important regulatory processes such as the regulation of sleep, mood and the degree of alertness and arousal.¹

The biological effects of NE in the synapse are primarily mediated by variations in the concentration of noradrenergic receptors and neurotransmitter. Whereas receptor concentrations may be regulated by desensitization, neurotransmitter concentrations are actively limited, in magnitude and duration, by NE transporter proteins (NETs).² NETs are localized pre-synaptically on noradrenergic nerve terminals, are activated upon polarization and recover about 70 to 90% of released NE from the synapse.¹ Neurons are thus largely dependent on NETs for the efficient removal of synaptic NE,

which make them vulnerable to abnormalities in NET expression or pharmacological blockade of these proteins.

NET and Psychobiology

Abnormalities in the central noradrenergic system have been implicated in the pathophysiology of several neuropsychiatric and neurodegenerative disorders, such as anxiety disorder,³ attention deficit hyperactivity disorder (ADHD),⁴ depression,^{5,6} drug abuse⁷ and Alzheimer's disease.⁸ More specifically, decreased levels of NETs have been observed in the brains of patients with major depression^{5,6} and Alzheimer's disease.⁸ Increased levels of NETs have been observed in the brains of rhesus monkeys upon chronic self-administration of cocaine.⁷ Given the implication of NETs in the abovementioned disorders, significant efforts have been directed from the pharmaceutical industry to develop potent and selective NET inhibitors.

NET inhibitors have been most widely used as antidepressants.⁶ The treatment of depression by alterations of synaptic monoamine concentrations was introduced in the 1950s. In 1957, Kuhn presented data from clinical trials of a tricyclic antidepressant drug, which had its efficacy partly based on NET inhibition (imipramine, (Tofranil®)).⁹ The same year, Loomer *et al.* reported clinical evidence for iproniazid, another type of antidepressant based on inhibition of monoamine oxidase (MAO), which is the enzyme responsible for metabolism of NE and serotonin (5-HT).¹⁰ Until the development of the selective serotonin transporter (SERT) inhibitors (a.k.a. SSRI's, e.g. Prozac®) in the 1980s, tricyclics and MAO inhibitors were predominantly used in antidepressant treatment. More recently, a hypothesis has been developed that NET and SERT inhibitors treat different kinds of depression and may be used concomitantly with benefits to the patient.¹¹

Whereas the noradrenergic system appears to play a central role in depression, inhibition of NETs in the treatment of ADHD has been suggested to be primarily related to the modulation of dopaminergic levels in the prefrontal cortex.¹² Such a mechanism is reasonable for two reasons. First, the concentration of dopamine transporters (DATs) in the prefrontal cortex is low.¹³ Second, dopamine (DA) has higher affinity for NET than NE itself.¹⁴ Both these facts together imply that NET may also accept DA as a substrate in brain regions devoid of DATs, which adds an extra dimension to the elucidation of the underlying mechanisms of other neuropsychiatric disorders in which NET is the target for treatment.

Brain Imaging in Studies of Neuropsychiatric Disorders

There are several techniques that allow non-invasive imaging of the living human brain. These can be divided into two fundamentally different classes of technique. One class, which provides anatomical information of the human brain, comprises imaging techniques such as magnetic resonance imaging (MRI) and X-ray computed tomography (CT). The other class, which provides functional information of the human brain, comprises tomographic methods such as positron emission tomography (PET) and single photon emission tomography (SPET).¹⁵ The latter two techniques require process-specific radioabelled probes (radioligands) to be administered before

the tomographic measurement is performed. When comparing PET and SPET, PET has the advantage of higher spatial resolution (3.8 mm for the PET camera used in this thesis project, vs. 8 mm for SPET) and better means of quantification (due to more accurate scatter and attenuation correction).

Brain imaging with PET is today a recognized tool in clinical studies of neuropsychiatric disorders and in drug development. The first quantitative study of dopamine D₂ receptor occupancy in relation to antipsychotic drug-treated patients was made 20 years ago with [¹¹C]raclopride¹⁶ Since then, PET has been proven useful for optimization of clinical treatment¹⁷ and proof of concept studies.¹⁸ A major advantage of PET within drug development is that detailed information regarding biodistribution and metabolism of a new drug can be obtained after administration of only a few micrograms. Thus, information regarding the success or failure of a new drug may be available before entering into large-scale clinical trials, which are costly and time-consuming.¹⁹⁻²¹

Although the scope of PET is great, there are some limitations with the technique, which need to be addressed for PET imaging facilities. PET cameras measure emission from annihilation events and thus require ligands labelled with positron-emitting radionuclides. The radionuclides used in this thesis, ¹¹C (*t*_{1/2} = 20.4 min) and ¹⁸F (*t*_{1/2} = 109.8 min), were produced in a cyclotron adjacent to the PET camera, due to their short half-lives. Large investments are required in equipment such as the cyclotron, PET camera, 'hot-cells' and other radiochemistry laboratory equipment, which so far has hampered the widespread use of PET. In contrast, the commonly used SPET radionuclide, ^{99m}Tc, can be obtained more inexpensively from commercially available generators.

A PET imaging study depends strongly on the radioligand used in the emission measurement. Generally speaking, a useful PET radioligand is specific for a certain protein or biological process. In this thesis, the focus has been on developing a radioligand specific for visualizing a brain neurotransmitter transporter. However, other proteins that may be visualized and measured include enzymes and receptors. Examples of biological processes that may be visualized by PET are metabolism and blood flow.

Radioligand Development

Factors that determine the success of a candidate PET radioligand are similar to those that govern the success of a candidate drug. For example, suitable *pharmacodynamic* properties, such as high *affinity* and *selectivity* for the target protein, are of great importance in both cases and thus make many existing drugs suitable candidate radioligands. However, it has also been shown that it is far from certain that a useful drug will be useful as a radioligand.

In PET radioligand development, the density of target proteins (*B*_{max}) is a key issue that need to be considered beforehand, as this will dictate the degree of affinity (*IC*₅₀, *K_i* or *K_d*) and selectivity that will be required from a successful candidate. The target protein density (*B*_{max}) should clearly exceed radioligand affinity (*K_d*) for good image contrast. Hence, a ratio of five between these two parameters can be used as a useful

initial guideline. The B_{max} of NETs in human insular cortex is about 4.4 pmol/g,²² which dictates that the affinity of a suitable radioligand for visualizing NETs in this region should be 0.9 nM. Other regions of the primate brain that are more dense in NETs, like the locus coeruleus (LC),^{23,24} may however be visualized by radioligands with lower affinity. In this manner, thresholds may be placed with regards to the minimum affinity required for imaging a target protein region by PET *in vivo*. However, species differences in the expression of NETs exist and these estimates should not be extrapolated across species.^{24,25} In addition, because affinity values may vary greatly in the literature depending on the assay conditions, it may be wise to not use these thresholds strictly. In this thesis work, it was decided that structures in the low nano-molar range should be evaluated in the original screening phase to eliminate the possibility of missing out on potentially useful NET radioligands.

The affinity of a radioligand will also influence its *in vivo* binding kinetics. For example, a high affinity radioligand will require a longer time to equilibrate than a low affinity radioligand in a high-density target region (e.g. [¹¹C]raclopride vs. higher affinity [¹¹C]FLB-457).²⁶ Radioligands showing slow kinetics (i.e. those that do not reach a peak equilibrium of specific binding within 90 min) may be advantageously labelled with fluorine-18 due to the longer half-life of this radionuclide. The peak equilibrium of specific binding is an asset in the biomathematical modelling of PET data. This concept will be discussed in more detail later.

The *selectivity* of a candidate radioligand is related to non-target protein densities. In the case of NET radioligands, the selectivity versus DATs is of central interest, since the DAT proteins are highly abundant in brain. [¹¹C]Cocaine for example, despite having a reported affinity of 640 nM for DATs,²⁷ has been used to image DATs in human striatum.²⁷ The selectivity of a candidate radioligand vs. SERT is not nearly as crucial, since the density SERTs in rat hypothalamus (a high density SERT region) is about three times that of NET in the LC of the rat brain.^{25,28,29}

Whereas the *in vitro* pharmacodynamic properties, affinity and selectivity, are the most important predictors in the selection of a candidate radioligand for PET evaluation, the *pharmacokinetic* properties of a candidate radioligand may only be determined by *in vivo* experiments. However, there are some guidelines (e.g. the "Lipinski's rule of five", *vide infra*) that have been shown to be useful in drug development that may also be successfully applied in the development of radioligands.

Radioligands are predominantly administered by intravenous injection. Thus, the *absorption* of a radioligand is achieved directly into the blood stream for efficient delivery to the target organ, which in this thesis was the brain. The *bio-distribution* of a CNS radioligand must be such that at least 2% of the radioactivity is accumulated in brain after administration, to ensure proper counting statistics with the PET camera. Several factors govern the accumulation of candidate radioligands in brain, including binding to plasma proteins, rapid metabolism, rapid clearance from plasma or efficient exclusion from brain by efflux pumps.³⁰⁻³³ These factors are hard to predict, but some guidelines on the physicochemical properties of a candidate drug have been developed. According to Lipinski,³⁴ for good drug permeability and tissue absorption,

the molecular weight should not exceed 500 g/mol, the *LogP* should not exceed five, the number of hydrogen bond (H-bond) donors should not exceed five and the total number of hydrogen bond acceptors should be less than ten.³⁴ For CNS drugs, it has been argued that more stringent rules need be applied, with a maximum molecular weight of 450 g/mol and a maximum *LogP* of four.³⁵ Furthermore, a parabolic relationship has been shown between *LogP* and brain extraction in a series of small non-ionized molecules, where the maximum brain accumulation was observed with *LogP* values between three and four.³⁶ *LogP* is also often associated with non-specific binding, but given the heterogeneity of such interactions, no firm support is to be found of such relationships in literature. Given the importance of lipophilicity in brain extraction and its potential involvement in non-specific interactions, calculated *LogP* values (*cLogP*'s) were used as guidelines in the selection of potential candidate radioligands alongside the previously mentioned pharmacologic parameters, affinity and selectivity. It is important to emphasize that the lipophilicity of a candidate radioligand, especially when calculated with computer programs, should only be used as a guideline in radioligand development and not as a strict discriminator.

The *metabolism* of a suitable PET radioligand must be such that no BBB permeable radiometabolites are formed that may contribute to brain radioactivity, since the PET camera merely measures radioactivity and does not distinguish between radiochemical entities. If a radiometabolite enters brain, it may have detrimental effects on the quantification of the PET data, especially if the radiometabolite has some degree of target selectivity.³² An estimate of the relative lipophilicity of a formed radiometabolites, and thus its BBB permeability, as well as quantitative data on the rate of metabolism of a radioligand, can be obtained by radio-chromatography techniques such as thin layer chromatography (TLC) and/or high performance liquid chromatography (HPLC).³⁰ The latter, coupled with mass spectrometry, may be especially useful in the identification of radiometabolites.³⁷ To test whether radiometabolites are present in brain during PET measurement, *ex vivo* analyses of brain tissue extracts can be performed. Such experiments require the animal to be sacrificed after the radioligand is injected and are mostly limited to rodents, which may diminish the utility of the obtained results, as species differences in metabolism (especially in the rate of metabolism) may be significant.

Radiochemistry with Positron-Emitting Radionuclides

Due to the short half-life of the positron-emitters, a suitable PET radioligand should be amenable to rapid and automated labelling to minimize radiation exposure to production personnel. As a rule of thumb, radiosyntheses involving positron-emitters should be completed within three half-lives of their production. It is thus of advantage if the radiolabel is inserted in the last possible step of the radiosynthesis. Automated apparatuses have been developed that convert the most commonly used cyclotron-produced precursors, [¹¹C]carbon dioxide and [¹¹C]methane, into more reactive alkylating agents, such as [¹¹C]methyl iodide³⁸ or [¹¹C]methyl triflate,³⁹ which are the most frequently applied electrophiles in the synthesis of ¹¹C-labelled radioligands. Higher homologues of [¹¹C]methyl iodide (*e.g.* ethyl, propyl and butyl) are also

available through ^{11}C -carboxylation, reduction and iodination of the appropriate aliphatic Grignard reagent,⁴⁰ but are much less utilized as labelling agents. Other labelling agents used in ^{11}C radiochemistry include [^{11}C]carbon monoxide,⁴¹ [^{11}C]ammonium cyanide⁴² and ^{11}C -labelled acyl chlorides.^{32,43}

Synthesis apparatuses that use [^{18}F]fluoride ion in direct aliphatic or aromatic nucleophilic substitutions have also been developed and are commercially available.⁴⁴ By further manipulations of such modules, or by in-house developed modules, electrophilic agents such as [^{18}F]fluoromethyl bromide and [^{18}F]fluoroethyl bromide, or their sulfonate ester analogues, may also be prepared.⁴⁵⁻⁵¹ Electrophilic [^{18}F]fluorine may seem like an attractive labelling agent, but is not amenable for labelling of receptor or transporter ligands due to its low specific radioactivity (SR).⁵²

Depending on the affinity of the radioligand and the density of the target population, different requirements will be posed on the minimum SR that must be employed to ensure that a receptor or transporter population is not saturated by carrier (compound containing a corresponding stable isotope of the radionuclide). It is generally accepted that if PET imaging is to be conducted under “true tracer conditions”, less than 5 % of the target population should be occupied by carrier.⁵³

Preliminary Evaluation of a Candidate Radioligand

The preliminary evaluation of a new radioligand may be performed by different *in vitro*, *in vivo* or *ex vivo* techniques. New ligands with unknown pharmacological properties need first be assayed for affinity and selectivity *in vitro*. These parameters may be obtained by competition studies between the unlabeled candidate radioligand and a radioligand of known affinity in tissue or homogenate containing the target protein. A candidate radioligand with suitable pharmacological properties may then be subjected to *post mortem* human *in vitro* autoradiography,^{54,55} in which brain tissue sections are incubated with the candidate radioligand and the accumulation of radioactivity is developed onto a sensitive film or by a phosphor imager. This technique may give a hint on the potential utility of a candidate radioligand in human brain tissue before clinical studies, but sometimes requires a great deal of optimisation of incubation and washing conditions in order to work efficiently. It is thus not recommended to discard a candidate radioligand on the basis of high non-specific binding in a non-optimised autoradiography experiment. In contrast, if autoradiograms display low non-specific binding as well as accumulation in known high-density regions under such non-optimised conditions, they may be a good indication of the success of a candidate radioligand. Additional blocking experiments with pharmacologically known ligands for other receptor systems may also be performed to further establish the specificity of the candidate radioligand.

As a means to assess the potential utility of a candidate radioligand *in vivo*, PET imaging may be performed in rodents, but more preferentially in non-human primates. The ratio of radioactivity concentration between a region that is known to contain a high density of target protein to a region known to be devoid of target proteins is often used as a measure of the utility of a radioligand to visualize its target. The higher the ratio, the easier it is to detect discrete changes in target densities due to

drug occupancy or disease. The binding potential (i.e. B_{max}/K_d) of a radioligand in a given brain region is a quantitative estimate of the receptor concentration in that region. This parameter may be obtained from PET data by using kinetic or equilibrium modelling approaches, such as the transient equilibrium model.^{53,56,57} In the latter model, the non-specific concentration of a radioligand in brain is assumed to be the same as the concentration in a reference region in brain that is devoid of target proteins.⁵⁶ This is a simplification that is not always valid,⁵⁷ but was used in this thesis due to the lack of a measured arterial input function. Thus, the specific binding was estimated as the difference in radioactivity concentration between target and non-target regions. The specific binding peak equilibrium was defined as the time after injection when maximum specific binding occurred.

Before such biomathematical modelling, the specific binding *in vivo* needs to be determined by pharmacological challenges with ligands of known affinity and selectivity. *Pre-treatment* studies, in which a ligand of known affinity and selectivity is administered before the radioligand, can test the specificity of the candidate radioligand. *Displacement* studies, in which a ligand of known affinity and selectivity is administered after injection of the candidate radioligand, can also test the reversibility of the binding. In addition to these experiments, which in principle may be performed in any given species *in vivo*, genetically modified mice that lack expression of a specific protein (a.k.a. knock-out mice) are now available for many pharmacological targets and may be used to test the binding specificity *in vivo* and *in vitro*.⁵⁸ Knock-out mice are powerful tools to test *in vivo* specificity, but one must consider that species differences between rodents and primates may be operating when interpreting results from such studies.

In rodents, but also in some rare exceptions in non-human primates, *ex vivo* analyses of regional brain radioactivity distribution can be performed by excising and measuring the brain regions of interest (ROIs). Since the ROIs of a rat brain are small in nature, such measurements may be advantageous to PET measurements with respect to partial volume effects (PVE).⁵⁹ As previously mentioned, radiometabolite analysis is a crucial step in the evaluation of a candidate radioligand and may be advantageously conducted concomitantly with *ex vivo* analyses of rat brain regions.³⁰

NET Inhibitors

Inhibitors of NE reuptake can be divided into subclasses depending on the number of fused rings in the molecular structure. The tricyclic antidepressants form an important group of antidepressants that comprises several potent and selective NET inhibitors.^{60,61} Other groups, in which potent NET inhibitors may be found are monocyclics,⁶²⁻⁶⁵ bicyclics⁶⁶ and tropane derivatives.^{67,68}

The mutual structural elements of all potent NET inhibitors (except tropanes) are two aryl rings (A and B, Fig. 1)) and a secondary amine. It has been suggested that the aryls should have an antiperiplanar orientation to the secondary amine nitrogen for optimal activity.⁶⁶ If an aliphatic H-bond acceptor (e.g. ether linkage or hydroxyl group) is present in the ligand, the stereochemical orientation of this moiety is of importance for affinity.^{63,64,66,69} For example, the enantiomers (*R*)-tomoxetine and (*S*)-

hydroxymaprotiline (OXA) inhibit NE reuptake with eudismic ratios of about 8 and 1000, respectively.^{61,64} Regarding aromatic substitution, 3'-chloro substitution of phenyl B seems to be optimal,^{63,66,70} whereas the optimal substitution of phenyl A is unclear. Tricyclic derivatives are generally unsubstituted in this ring, whereas the rank order of pharmacological activity on the nisoxetine platform is 2-I > 2-SMe > 2-Me > 2-OMe.^{64,71} It has been shown that replacing the 2-ethoxy group in reboxetine with a 2-methoxy group results in increased potency.⁶³ Since the reboxetine and nisoxetine platforms are very similar, it is likely that the reboxetine platform would follow the same pattern as the nisoxetine platform in the rank order of potency regarding substitution of phenyl A. However, no such structure-activity relationships (SAR) have been reported to date.

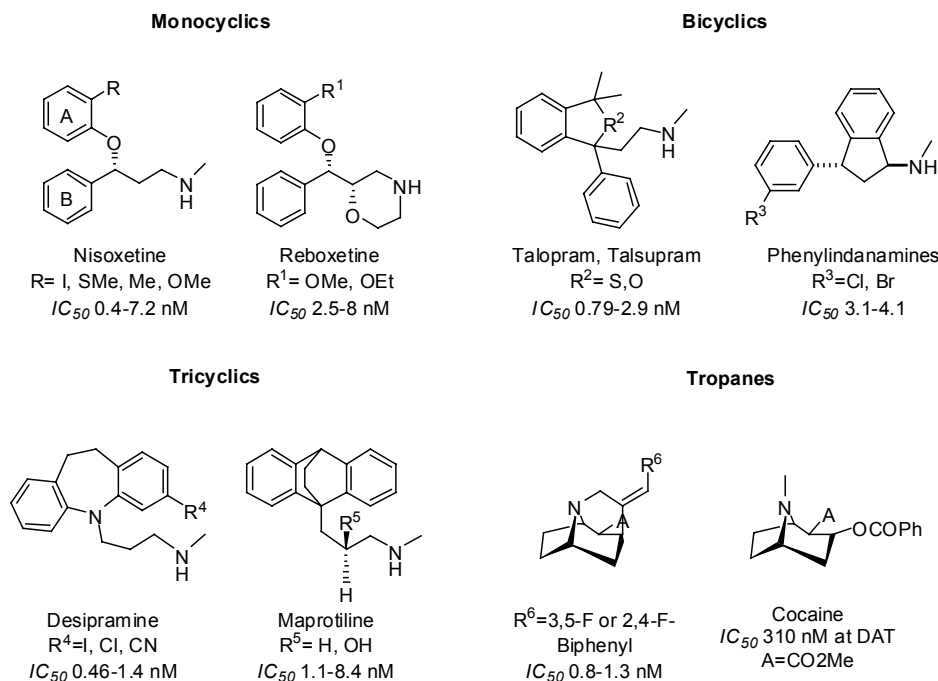


Figure 1. Structures and affinities of various structural classes of NET inhibitors.

By estimating the lowest energy conformation of eleven of the most potent NET inhibitors ($IC_{50} < 10$ nM) derived from the structural classes depicted above by using Spartan (Wavefunction Inc., Irvine CA, USA), the distances between the three binding sites were calculated. No attempt was made to correlate distances with affinity for NET, since the compounds were not screened against their *in vitro* affinity in the same assay. The mean distance between centroids within the two phenyls was 4.98 ± 0.45 Å, whereas the distances between centroids within phenyl A and B to the nitrogen atom of the secondary amine were 5.65 ± 0.53 Å and 6.40 ± 0.58 Å, respectively. These parameters (together with the angles between the binding sites)

were used to make crude predictions on whether new ligands would possess high affinities towards NET.

AIMS AND LONG TERM OBJECTIVES

This project aimed to develop the first effective radioligand for imaging NET in the living human brain. First, because the predictive capacity of physicochemical parameters on the success of candidate radioligands *in vivo* may be limited, potent NET inhibitors from diverse structural classes were to be prepared and evaluated as candidate NET radioligands. Second, in the event of any successful candidate radioligand, that compound would be subjected to further structural modifications.

In the long term (not included in this thesis work), a suitable NET radioligand would offer the possibilities to:

- i) examine the distribution and density of NETs in the living human brain, both in healthy volunteers and in patients with the neuropsychiatric disorders, especially depression.
- ii) identify and validate targets for drug action in neuropsychiatric disorders by brain imaging in drug treated patients.
- iii) develop principles for optimal clinical treatment.

The outcome of these examinations could subsequently be applied in the development of more effective drugs.

RESULTS & DISCUSSION

When this project was started, only one candidate radioligand had been evaluated as a PET radioligand for imaging central NETs, namely [^{11}C]nisoxetine.⁷² Although [^3H]nisoxetine had long been a validated tool for *in vitro* autoradiographic studies of NETs,^{5,25,73,74} its isotopomer [^{11}C]nisoxetine exhibited a high degree of non-specific binding *in vivo*, which diminished its utility as a PET radioligand.⁷²

Bicyclic and Tricyclic NET inhibitors as PET radioligands (Paper I)

A series of phenyl phthalans were discovered as potent monoamine transporter inhibitors by Bøgesø et al. at the Danish pharmaceutical company, Lundbeck.⁶⁶ Among these compounds, two NET inhibitors, talopram and talsupram, were further evaluated in clinical trials, in which they demonstrated some antidepressant efficacy.^{75,76} Talopram and talsupram are two of the most potent NET inhibitors reported to date with IC_{50} 's of 2.9 and 0.79 nM, respectively. Furthermore, they are highly selective (>100-fold) versus a wide range of other targets.

Desmethylinipramine (desipramine, DMI) is the *N*-desmethyl metabolite of the tricyclic antidepressant, imipramine (IMI, Tofranil®).⁹ In contrast to IMI, which is a selective and potent SERT inhibitor, DMI is a potent and selective NET inhibitor,⁶⁰ with a NET affinity of 0.97 nM (IC_{50}).⁷⁰ DMI has been widely used as an antidepressant.⁶ The clinical side effects of tricyclics are usually associated with their

affinity towards muscarinic acetylcholine receptors. DMI, however, has only a low affinity for these receptors ($K_i = 66$ nM)⁷⁷ that is of minor importance in relation to PET imaging. Before this study, the isotopomer [³H]DMI had been used for *in vitro* autoradiography of NETs in the human brain *post mortem*.^{78,79} [³H]DMI was found to distribute heterogeneously in the human brain, with binding to two different sites, of which that of higher affinity was assumed to be the NET binding site.⁷⁸

Given that the physicochemical properties of DMI, talopram and talsupram were in the range expected for a suitable PET radioligand for NET, and that the clinical efficacy of all three ligands demonstrated that they gain entry to brain, we were led to evaluate the three compounds as candidate radioligands for NET.

Chemistry

With the co-operation of Lundbeck A/S, non-radioactive precursors and standards for the ¹¹C-labeling of talopram and talsupram in their *N*-methyl positions were obtained. The nor-methyl precursor for DMI was readily obtained by following the synthetic route reported by Van Dort et al.⁸⁰

The labelling of secondary amines using [¹¹C]methyl triflate is well described in the literature.^{39,81} Using such established conditions, the radiochemical yields (RCYs) of [¹¹C]DMI, [¹¹C]talopram and [¹¹C]talsupram (Fig. 2, *vide infra*) from [¹¹C]methyl triflate were in the order of 60%. The SRs of [¹¹C]DMI, [¹¹C]talopram and [¹¹C]talsupram were between 58 and 75 GBq/μmol, respectively, which is in the range usually achieved when using [¹¹C]methyl iodide derived from target produced [¹¹C]carbon dioxide.⁸²

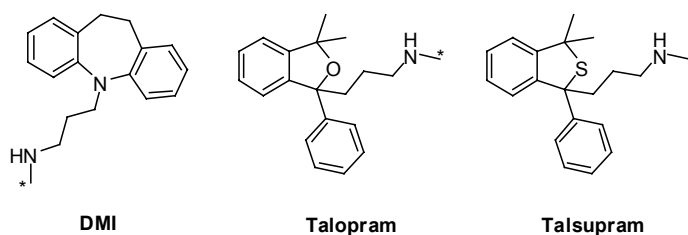


Figure 2. Structures of the NET inhibitors DMI, talopram and talsupram. The asterisk denotes the labelling position. Racemic talopram and talsupram were evaluated in this study.

PET in Non-human Primates

The regional radioactivity distribution in brain after injection of [¹¹C]talopram or [¹¹C]talsupram into a cynomolgus monkey was slightly heterogeneous, with higher accumulation of radioactivity in NET-rich regions (*e.g.* lower brainstem) than in NET-poor (*e.g.* striatum). The global radioactivity accumulation in brain was however very low, with maximally 0.7 and 1.3% of the injected radioactivity present in the monkey brain after injection of [¹¹C]talopram or [¹¹C]talsupram, respectively. This low accumulation in brain, which is too low for a useful CNS PET radioligand, was also confirmed by McConathy et al., who reported that about 0.07% of the

injected dose (%I.D.) per g of the active enantiomers of [^{11}C]talopram and [^{11}C]talsupram entered brain.⁸³ It may seem like a large discrepancy that these radioligands failed to accumulate in brain, since previous data suggested that the ligands had clinical efficacy as antidepressants.^{75,76} A number of factors may limit the access of a radioligand to brain (see page 12), of which some are saturable processes. A reasonable explanation for these diverse observations is that talopram and talsupram take part in such saturable processes, making their availability in brain concentration dependent. Examples of such processes are binding to plasma proteins (e.g. serum albumin) or active exclusion from brain by a brain efflux pump (e.g. Pg-P).

After injection of [^{11}C]DMI into a cynomolgus monkey, radioactivity readily entered brain (2.7%I.D.). The regional distribution of radioactivity in brain was however only slightly heterogeneous and quite insensitive to inhibition of NETs by pre-treatment with the reference NET inhibitor, DMI. This was in contrast to previous *in vitro* studies with [^3H]DMI.⁷⁹ An explanation for this discrepancy is that washing steps, that may only be utilized *in vitro*, remove non-specific binding in the autoradiography experiments. Another possible explanation is that species differences exist in the expression of NETs between the human and the non-human primate brain.

Radiometabolite Analysis

The metabolism of [^{11}C]DMI, [^{11}C]talopram and [^{11}C]talsupram was comparatively fast, with about 20 - 25% of radioactivity in plasma represented by parent radioligand at 45 min after injection. No radiometabolites more lipophilic than their parent compounds were found in plasma. It is thus unlikely, although not impossible, that radiometabolites entered brain and confounded brain imaging with any of the evaluated radioligands.

Candidate Radioligands Based on Aryloxy Morpholines (Papers II-V)

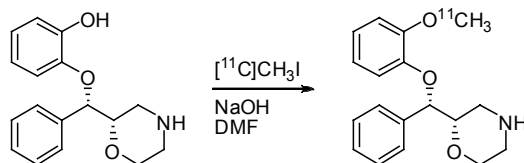
Reboxetine (Edronax®) is one of few second generation antidepressants that target NET in contrast to SERT.⁸⁴ In the original paper on the development of reboxetine, its *O*-methyl *desethyl* analog (MeNER, $\text{IC}_{50} = 2.5\text{nM}$) was found to be about threefold more potent than reboxetine itself in the inhibition of NETs in rat cortical synaptosomes.⁶³ Because of its two chiral centers, there are four stereoisomers of reboxetine. Of these, the *S,S*-isomer is the most potent, with a eudismic ratio of about 20 *in vitro* compared to its *R,R*-enantiomer.⁸⁵

In view of: i) the high affinity and selectivity of (*S,S*)-MeNER for NET, ii) the comparatively low lipophilicity of (*S,S*)-MeNER compared to reboxetine, and iii) the relative ease of labelling the *O* methyl group of (*S,S*)-MeNER with carbon-11, (*S,S*)-MeNER was chosen as a candidate radioligand for NET.

Radiochemistry

The *O-desmethyl* non-labelled precursors (NER; individual *syn* enantiomers) for MeNER were obtained with the co-operation of Eli Lilly & Co.

Due to competitive alkylation of the morpholino moiety of NER, variable amounts of *N*-alkylated product were observed when using [^{11}C]methyl triflate as labelling agent for MeNER, except when the precursor was *N*-Boc protected. In contrast, MeNER could be regiospecifically labelled in its *O*-methyl position when using [^{11}C]methyl iodide under alkaline conditions (Scheme 1).^{86,87} With such conditions, the individual *syn* enantiomers of [^{11}C]MeNER were prepared in quantitative RCY from [^{11}C]methyl iodide and at high SR (48-74 GBq/ μmol).



Scheme 1. Labelling of (*S,S*)-MeNER in its *O*-methyl position with ^{11}C .

PET in Non-human Primates

Following injection of [^{11}C]MeNER, radioactivity readily entered brain ($\sim 3\%$ I.D.). The binding of [^{11}C]MeNER to NETs in the cynomolgus monkey brain was found to be highly stereospecific, with the highest retention of radioactivity in NET-rich regions after injection of the (*S,S*)-isomer (Fig. 3).

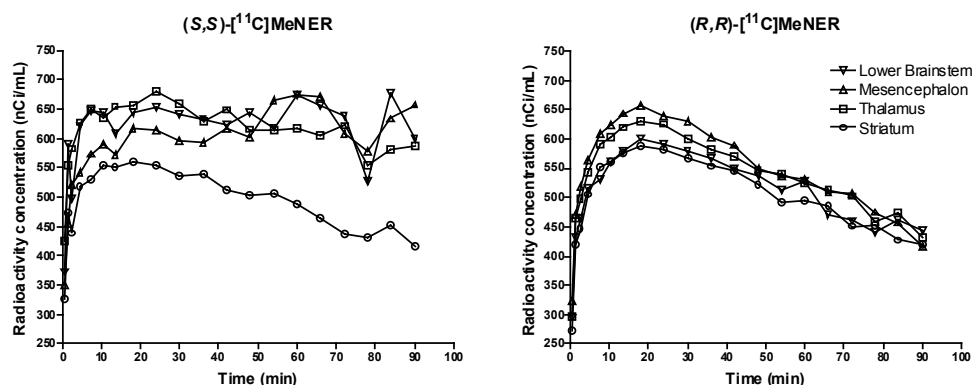


Figure 3. Regional brain distribution of radioactivity after injection of the individual *syn* (*S,S* and *R,R*) enantiomers of [*O*-methyl- ^{11}C]MeNER.

In a pre-treatment experiment with DMI, the specific binding was markedly decreased in the examined brain regions, almost to a striatal level (Fig. 4). The specific binding of (*S,S*)-[^{11}C]MeNER increased towards the end of the PET measurement and thus failed to reach a transient equilibrium during the time-frame of the PET study (93 min).⁵⁶

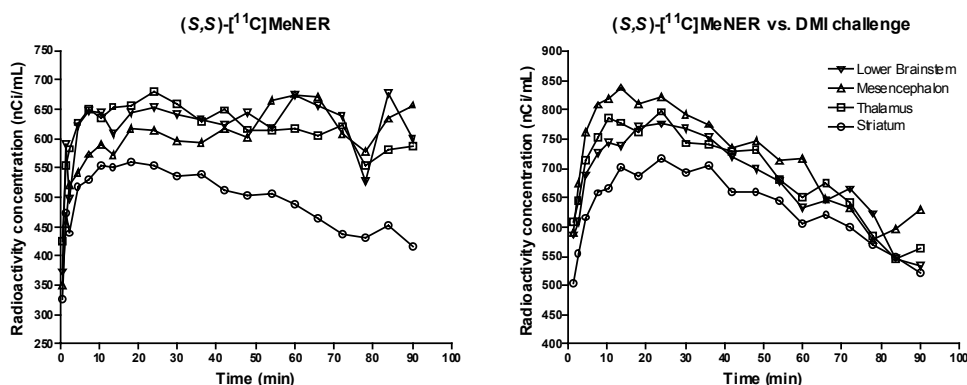


Figure 4. Regional brain distribution of radioactivity in PET experiments with (S,S) - $[^{11}\text{C}]\text{MeNER}$ under baseline (left) and pre-treatment conditions (right).

A slight increase in the global brain radioactivity accumulation was observed in the pre-treatment experiment with DMI. This increase may have been due to inhibition of peripheral NETs and/or radioligand metabolism,⁸⁸ which may both increase the plasma concentration of a radioligand.

In vitro Autoradiography

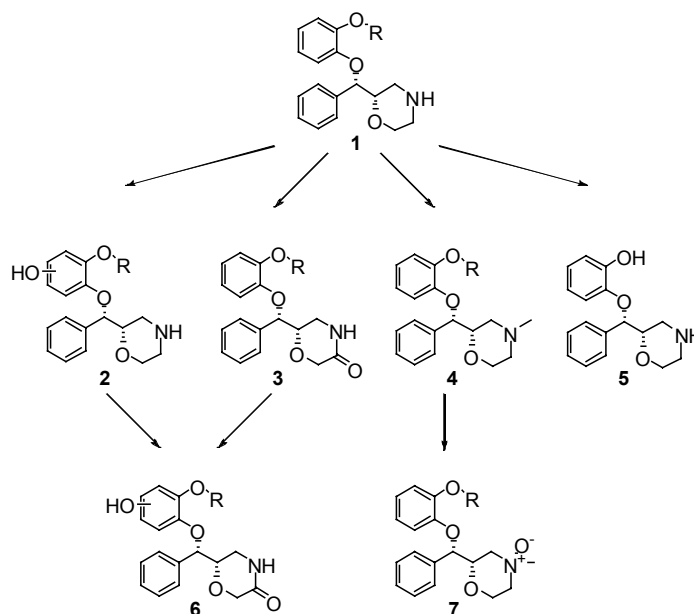
In a preliminary autoradiography experiment with (S,S) - $[^{11}\text{C}]\text{MeNER}$ on *post mortem* human brain cryosections, radioactivity accumulated in the LC, a region known to be dense in NETs both in the brains of rats and humans.^{23,25,73} However, the non-specific binding of (S,S) - $[^{11}\text{C}]\text{MeNER}$ was also high throughout the entire brain section under these non-optimised conditions.

Autoradiography experiments with (S,S) - $[^3\text{H}]\text{MeNER}$ in normal and NET knock-out mice showed negligible amounts of specific binding in the knock-outs, whereas high binding was found in NET-rich regions of normal mice.⁵⁸ This further supported the specific binding of (S,S) -MeNER to NET.

Analysis of Metabolites of (S,S) - $[^{11}\text{C}]\text{MeNER}$ in Rats, Monkeys and Humans (Paper VII)

In view of the positive results obtained with (S,S) - $[^{11}\text{C}]\text{MeNER}$, together with other separate reports by the PET groups at both Toronto and Brookhaven,^{86,87} it was decided to assess the utility of (S,S) - $[^{11}\text{C}]\text{MeNER}$ for the determination of reboxetine-induced central NET inhibition in healthy human volunteers. Concurrent with these PET studies, we also performed radiometabolite analysis. Thus, in paper VII, we evaluate the metabolism of (S,S) - $[^{11}\text{C}]\text{MeNER}$ in humans, monkeys and rats.

The metabolism of reboxetine has been studied extensively by Dostert et al.⁸⁹ Due to the high structural similarity between MeNER and reboxetine, we hypothesized that the biotransformations of the two compounds would be similar (Scheme 2).



Scheme 2. Putative metabolism of MeNER (R = Me) based on the metabolism of the *O*-ethyl homologue, reboxetine (R = Et).⁸⁹

Reboxetine (**1**, O = Et) undergoes extensive oxidative metabolism in all species, through three major metabolic pathways: i) hydroxylation of the ethoxy-bearing aryl ring (**2**), ii) oxidation of the morpholinyl moiety (**3**) and iii) *O*-de-ethylation (**5**). Another possible pathway for metabolism was found to be *N*-methylation (**4**) followed by oxidation to form the *N*-oxide, **7**.⁸⁹

Consistent with literature on the metabolism of reboxetine,⁸⁹ it was found that the metabolism of (*S,S*)-[¹¹C]MeNER was faster in rats ($17 \pm 4\%$ at 30 min, $n = 3$) than in monkeys ($77 \pm 14\%$ unchanged radioligand at 30 min, $n = 5$) and humans ($85 \pm 7\%$ at 30 min, $n = 18$). Two other radiometabolites were found in monkey and human plasma, with one more lipophilic than (*S,S*)-[¹¹C]MeNER itself. In humans, this radiometabolite comprised $9 \pm 5\%$ of the plasma radioactivity at 4 min and $1 \pm 2\%$ at 40 min. In monkeys, the same radiometabolite was only detectable in the first plasma sample, where it comprised $3 \pm 2\%$ of the total radioactivity. No radiometabolite more lipophilic than MeNER was observed in rat plasma. In rat brain *ex vivo*, most of the radioactivity ($> 87\%$) corresponded to (*S,S*)-[¹¹C]MeNER. De-methylated, and thus unlabeled, **5** was the major metabolite identified by LC-MS and has no implication for PET studies with (*S,S*)-[¹¹C]MeNER.

Our findings imply that radiometabolites will have insignificant or no effect on brain PET imaging in rats and monkeys. In human subjects, significant amounts of a transient lipophilic metabolite were detected in plasma. The kinetics of this radiometabolite appears favourable to successful PET imaging, as this radiometabolite is rapidly cleared. However, it cannot yet be wholly excluded that

this radiometabolite has a detrimental effect on imaging of NETs in the human brain with (S,S)-[¹¹C]MeNER.

Fluorinated Analogues of (S,S)-MeNER (Paper III)

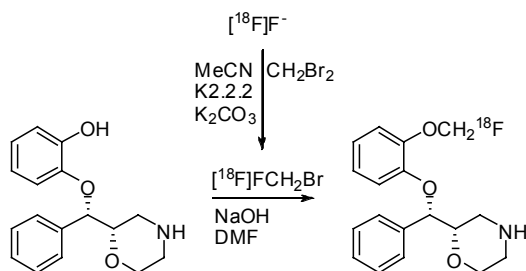
In the clinical evaluation of (S,S)-[¹¹C]MeNER, the test-retest variability in BP ranged between 17 and 31%, depending on the examined ROI.⁹⁰ This variability is too large for measurements of discrete changes of NET inhibition in brain. The large test-retest variability is primarily associated with the slow binding kinetics of the radioligand, which necessitates binding potentials to be estimated from emission data obtained between 63 and 93 min after injection of (S,S)-[¹¹C]MeNER. At these time-points, the data is very vulnerable to noise due to the short half-life of ¹¹C. In an attempt to extend data acquisition over the specific binding peak equilibrium, we were interested in introducing a longer-lived radionuclide into the structure. Around this time period, it had been demonstrated that an aryl *S*-fluoromethyl SERT radioligand, (S)-[¹⁸F]fluoromethyl-(+)-McN5652, displayed a similar binding affinity and regional brain distribution as its *S*-methyl analogue.⁹¹ In addition, the radiochemistry of the radiofluoromethylation agents, [¹⁸F]bromofluoromethane and [¹⁸F]fluoroiodomethane, had also been recently revisited.^{45,50,51,78}

We hypothesized that an *O*-[¹⁸F]fluoromethyl analogue of (S,S)-[¹¹C]MeNER ((S,S)-[¹⁸F]FMeNER) would i) be readily available from its *O*-desmethyl precursor, NER, the same non-labelled precursor that is used in the preparation of (S,S)-[¹¹C]MeNER, ii) have similar binding affinity as (S,S)-[¹¹C]MeNER, and iii) allow imaging of the specific binding peak equilibrium and thus also provide a more robust estimate of NET density in the primate brain.

Radiochemistry and Pharmacology

In a pharmacological assay, (S,S)-FMeNER was found to be almost equipotent to (S,S)-MeNER, with an *in vitro* affinity of 3.1 nM (*K_i*), compared to 2.5 nM for (S,S)-MeNER. (S,S)-FMeNER had also retained its selectivity towards NET.

(S,S)-[¹⁸F]FMeNER was prepared from [¹⁸F]fluoride ion in a two-step process (Scheme 3). First, [¹⁸F]fluoride ion was reacted with dibromomethane to yield [¹⁸F]fluoromethyl bromide, which was purified by distillation through silica Sep-paks.⁴⁶ In the second step, [¹⁸F]fluoromethyl bromide was reacted with the non-labelled phenolic precursor of (S,S)-[¹⁸F]FMeNER. The overall yield of this unoptimized two-step process was around 5 to 10% and the SR was between 110 and 185 GBq/μmol. Further improvements in this process have been made since it was originally reported, which has increased the yield to 13%.



Scheme 3. Preparation of (*S,S*)-[^{18}F]FMeNER starting from cyclotron-produced [^{18}F]fluoride ion.

PET in Non-Human Primates

In PET measurements with (*S,S*)-[^{18}F]FMeNER, radioactivity entered brain to a similar extent as in PET measurements with (*S,S*)-[^{11}C]MeNER (2.8% I.D.). Radioactivity also distributed similarly within brain, with DMI-sensitive binding in the lower brainstem, mesencephalon and thalamus. Furthermore, the specific binding reached peak equilibrium at 90 to 120 min after injection. However, there was also an accumulation of radioactivity in the cortical regions, which was insensitive to DMI. This phenomenon had earlier been observed for other ^{18}F -labelled radioligands and had been ascribed to accumulation of [^{18}F]fluoride ion in bone (in this case, the skull) and ‘spill-over’ of radioactivity through the PVE into adjacent regions (in this case, cortex).⁹²

While this work was in progress, Hamill et al. showed that the *in vivo* defluorination rate could be decreased by di-deuteration of the fluoromethylene moiety of the NK₁ receptor radioligand, [^{18}F]SPA-RQ.⁹³ In the light of those results, we decided to prepare (*S,S*)-[^{18}F]FMeNER-D₂ as a metabolically more stable analogue of (*S,S*)-[^{18}F]FMeNER.

Radiochemistry

A similar process was used in the preparation of (*S,S*)-[^{18}F]FMeNER-D₂ as in the synthesis of (*S,S*)-[^{18}F]FMeNER, except that dibromoethane-*d*₂ was employed in the first step of the radiosynthesis. Similar yields and specific radioactivities were thus observed for (*S,S*)-[^{18}F]FMeNER-D₂ as for (*S,S*)-[^{18}F]FMeNER.

PET in Non-Human Primates

The regional distribution of radioactivity in monkey brain after injection of (*S,S*)-[^{18}F]FMeNER-D₂ was similar to that observed with the previously evaluated aryloxy morpholines (Fig. 5, *vide infra*). The binding was sensitive to pharmacological challenge with NET inhibitor, but not DAT or SERT inhibitors.

When comparing PET measurements with (*S,S*)-[^{18}F]FMeNER-D₂ and (*S,S*)-[^{18}F]FMeNER, three important observations could be made: First, the peak brain radioactivity was higher (3.6%I.D. vs. 2.8%I.D.) and occurred at a later time-point (12 min vs. 8 min). Second, the specific binding peak equilibrium was shifted

towards later time-points and did not occur until 120 to 160 min. Third, the accumulation in the upper arm bone (humerus) was reduced. This level reached a plateau at about 90 min, whereas it increased for the duration of the experiment with the non-deuterated radioligand.

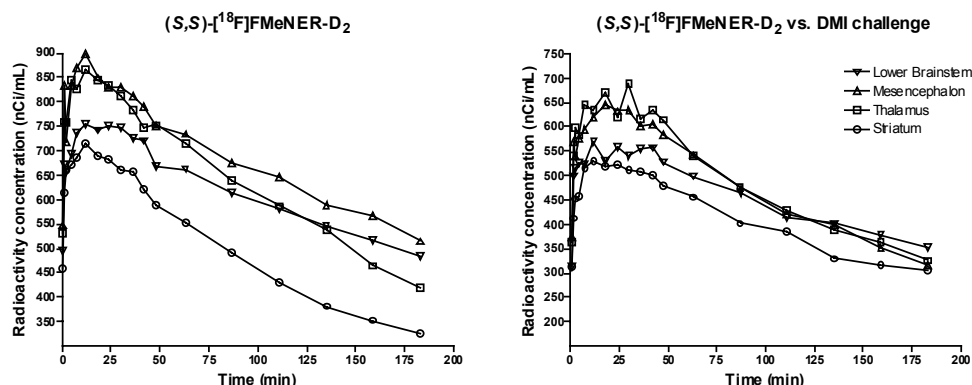


Figure 5. Time-activity curves derived from baseline (left) and pre-treatment (right) PET measurements with (S,S) - $[^{18}\text{F}]\text{FMeNER-D}_2$.

Radiometabolite Analysis

All three observations above imply that the plasma half-life of the radioligand was increased by a deuterium effect,⁹⁴ but this was not confirmed by radiometabolite analysis. The metabolism of (S,S) - $[^{18}\text{F}]\text{FMeNER-D}_2$ and (S,S) - $[^{18}\text{F}]\text{FMeNER}$ was found to be similar, with about 85% of radioactivity in plasma as parent compound at 45 min and 76% at 90 min. Radiometabolites more lipophilic than parent were not detected in monkey plasma. However, (S,S) - $[^{18}\text{F}]\text{FMeNER-D}_2$ and (S,S) - $[^{18}\text{F}]\text{FMeNER}$ are expected to undergo similar metabolism as (S,S) - $[^{11}\text{C}]\text{MeNER}$.

In vitro Imaging of NET using (S,S) - $[^{18}\text{F}]\text{FMeNER-D}_2$ (Paper IV)

In paper IV, an *in vitro* autoradiographical evaluation of the binding of (S,S) - $[^{18}\text{F}]\text{FMeNER-D}_2$ to *post mortem* human brain cryosections was performed. The aims of this study were to evaluate the specificity of binding to human brain tissue, as well as attempting to visualize NETs external to the high-density regions LC and raphe nuclei (RN).

In vitro imaging of NETs had earlier been performed in human brain tissue with $[^3\text{H}]\text{DMI}$,^{78,79} $[^3\text{H}]\text{mazindol}$ ²³ and $[^3\text{H}]\text{nisoxetine}$.^{5,8,73} Of these radioligands, $[^3\text{H}]\text{nisoxetine}$ has been the most suitable to examine NETs within the human LC and RN but no other regions.^{5,8,73} An attempt at imaging NETs with $[^3\text{H}]\text{nisoxetine}$ by whole human hemisphere autoradiography had failed in imaging NETs external to the LC (Hall *et al.*, unpublished results).

Autoradiograms labelled with (S,S) - $[^{18}\text{F}]\text{FMeNER-D}_2$ showed the highest levels of specific binding in the LC, followed by markedly lower levels in the cerebellum, thalamus and temporal cortex (Table 1, *vide infra*). Negligible levels of specific binding were seen in the occipital cortex and striatum. The binding of

(*S,S*)-[^{18}F]FMeNER-D₂ was unaffected by co-incubation with the selective DAT and SERT inhibitors PE2I⁹⁵ and citalopram,⁷⁰ respectively, which indicated that the binding was selective to NET.

Table 1. A semi-quantitative analysis of the binding of (*S,S*)-[^{18}F]FMeNER-D₂ to *post mortem* human brain tissue.

	Specific binding related to locus coeruleus			Specific binding / total binding		
	Percent	s.e.m.	n	Per cent	s.e.m.	n
Locus coeruleus	100.0		4	47.1	7.2	4
Pons anterior	9.8	4.9	4	7.0	2.1	4
Caudatus	5.7		1			
Putamen	3.0		1			
Thalamus	8.0		1			
Temporal cortex	12.3	4.3	4	7.8	2.7	4
Insular cortex	9.9		1			
Occipital cortex	1.6		1			
Cerebellum, total	15.2	5.0	4	9.9	2.1	4
Cerebellum, grey matter	15.6	6.0	4	8.4	2.6	4
White matter	7.6	4.3	5			

In conclusion, the binding of (*S,S*)-[^{18}F]FMeNER-D₂ to NET was found to be specific *in vitro*. The attempts at imaging regions external to LC failed, possibly because of lower densities of NETs in those regions. Although incubation conditions may be further altered to increase specific binding *in vitro*, it is unclear if (*S,S*)-[^{18}F]FMeNER-D₂ can be utilized in imaging NETs external to LC *in vivo*.

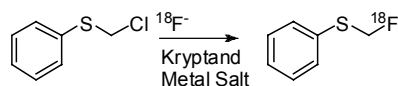
One-Pot Syntheses of [^{18}F]Fluoromethyl Ethers and Sulfides (Unpublished Results)

Radioligands containing aryl ^{18}F -fluoromethyl ethers, such as (*S,S*)-[^{18}F]FMeNER-D₂ (*vide supra*), have been extensively utilized in PET recently.^{46,51,91,96,97} Fluorine-18 has some general advantages over carbon-11, such as i) a longer half-life ($t_{1/2}$ = 109.8 vs. 20.4 min), which allows for longer data acquisition with PET radioligands that show slow kinetics, and ii) a lower positron energy (650 keV vs. 960 keV) which may increase the spatial resolution of PET measurements performed with radioligands labelled with ^{18}F . The latter is of particular importance for the imaging of small brain regions with the new high-resolution PET cameras (e.g. 2.2 mm).⁹⁸

The radiolabelling of aryl fluoromethyl ethers and sulfides has mainly been performed by alkylation of corresponding *desfluoromethyl* phenolic precursors with ^{18}F -labelled electrophiles. These electrophiles include ^{18}F -labelled fluoromethyl bromide⁴⁵⁻⁴⁷, fluoromethyl iodide^{50,51}, fluoromethyl mesylate^{48,49}, fluoromethyl triflate⁴⁶ and fluoromethyl tosylate^{48,49}. In all cases, a purification step has been

deemed necessary for the subsequent fluoroalkylation step. The overall yield of a radioligand labelled by this chemistry is usually in the range 15 to 20%.^{49,93,99}

As a means to increase the yields, and simplify reaction conditions, we were interested in attempting to synthesize the [¹⁸F]fluoromethyl ethers and sulfides by direct substitution with [¹⁸F]fluoride ion on corresponding chloromethyl precursors. Due to its commercial availability, chloromethyl phenyl sulfide was chosen as a model compound for the reaction.



Scheme 4. Labelling of aryl fluoromethyl ethers from α -chloromethyl ethers or sulfides.

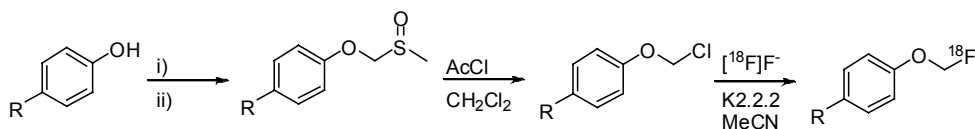
Synthesis of Aryl [¹⁸F]Fluoromethyl Sulfides

The yield of [¹⁸F]fluoromethyl phenyl sulfide was found to be dependent on temperature, time, kryptand (K2.2.2 or 18-crown-6) and the metal salt (cesium or potassium carbonate) used in the radiolabelling experiment (Scheme 4, *vide supra*). Yields ranged from 2 to 75% under the studied conditions. The highest yield (75%) was observed when heating a mixture of chloromethyl phenyl sulphide (0.27 M in acetonitrile), with the kryptand K2.2.2 (kryptofix®) and potassium carbonate as metal salt at 130°C for 40 min. The reaction time could be decreased to 10 min without reduced yield (74%) when using microwave-aided heating instead of thermal heating. Higher temperatures (in DMF and DMSO) and prolonged microwave heating had either a negative or no effect on the yield. Thus, the original radiochemical yield (RCY) of [¹⁸F]fluoromethyl phenyl sulfide was improved from 2 to 74% under these improved conditions.

Synthesis of Aryl [¹⁸F]Fluoromethyl Ethers

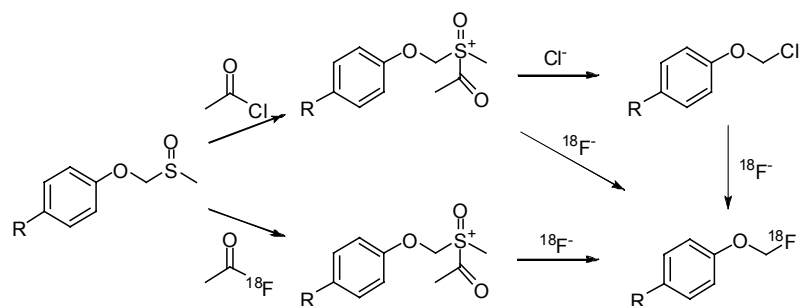
With the improved conditions established in the study of the preparation of [¹⁸F]fluoromethyl phenyl sulfide, we attempted labelling of fluoromethyl ethers by the same methodology. Various chloromethyl phenyl ethers have been described and are readily available from their corresponding phenols via a three step synthetic process.¹⁰⁰ As model compounds for this reaction, we chose to prepare one slightly electron deficient (*p*-chloro), one neutral (unsubstituted) and one electron-rich (*p*-methoxy) aryl chloromethyl ether.

Aryl chloromethyl ethers are known to decompose.¹⁰¹ It was also noted by us that phenyl chloromethyl ether decomposed on extended storage at 4 °C. As a means to circumvent this problem, we were interested in attempting to generate the aryl chloromethyl ether *in situ*. Thus, we were interested in introducing [¹⁸F]KF together with acetyl chloride in the last step of the synthesis (Scheme 5).



Scheme 5. Synthesis of aryl fluoromethyl ethers from their corresponding phenols. Reagents: i) $\text{ClCH}_2\text{SCH}_3$, NaI, NaH, DMF. ii) MCPBA, CH_2Cl_2 .

When generating the chloromethyl ether of *p*-chlorophenol *in situ*, an improved radiochemical yield (rcy) was observed (76%) compared to when the *p*-chlorophenyl chloromethyl ether was first isolated and then reacted with $[\text{}^{18}\text{F}]\text{KF}$ (67%). A possible explanation of this finding is that multiple reaction pathways may be operating in this one-pot method, all yielding the desired aryl fluoromethyl ether (Scheme 6, *vide infra*).



Scheme 6. Tentative mechanism for the transformation of sulfones into $[\text{}^{18}\text{F}]$ fluoromethyl ethers. $[\text{}^{18}\text{F}]\text{Acetyl fluoride}$ may be formed *in situ* from the reaction of $[\text{}^{18}\text{F}]$ fluoride with acetyl chloride.

The rank order for the radiochemical yield with the different substituents on the phenyl ring was *p*-methoxy (76%) > H (44%) > *p*-chloro (22%). This implies that the fluoridation of these aryls is dependent on the electron density in the phenyl ring. One reasonable explanation for this observation is that substrate stability is more important than reactivity, which if too high may lead to substrate decomposition. With electron donating groups on the aryl ring, an inductive effect on the oxygen of the chloromethyl ether moiety can decrease its electron withdrawing properties. This may stabilize the methylene carbon, which also has another electron-withdrawing group directly attached (the chlorine atom). An electron-withdrawing aryl ring might induce a larger relative positive charge on the methylene carbon, which may lead to higher reactivity.

A drawback with this method is that more synthetic work is required to produce the non-labelled precursors and that the overall yields are moderate from the corresponding phenols (~40%).¹⁰⁰ However, this method holds promise as an alternative direct substitution method for ^{18}F -fluoromethylations in which ^{18}F -labelled electrophiles do not need to be produced and isolated. Application of this method to

the ^{18}F -labelling of more complex structures (e.g. receptor radioligands, containing fluoromethyl moieties) will reveal the true utility of this method.

Hydroxylated Analogues of DMI and (*S,S*)-MeNER (Paper V)

The low specific binding observed in regions external to LC with (*S,S*)-[^{18}F]FMeNER- D_2 *in vitro* was ascribed to the low densities of NETs in those regions. It was thus concluded that the imaging of NET in low-density regions would require NET inhibitors with either higher affinity and/or lower non-specific binding. Although not clearly supported experimentally, the non-specific binding of a radioligand in brain *in vivo* is often considered to be associated with its lipophilicity. We were therefore interested to test whether a reduction in lipophilicity together with retained affinity towards NET of two potent NET inhibitors, (*S,S*)-MeNER and DMI (Fig. 6, *vide infra*), would decrease their non-specific distribution in the monkey brain *in vivo*.

By consideration of the analogous (*S*)-hydroxymaprotiline (OXA), a potent tricyclic NET inhibitor, it was hypothesized that the introduction of a hydroxyl group into the β -carbon of the aminopropyl side-chain of DMI might be tolerated. It was also hypothesized that stereoselectivity would be of high importance, since the binding of OXA to NET is highly stereoselective, with the *S*-enantiomer being the more potent with an eudismic ratio of about 1000.

Investigations of SAR on the aryloxy morpholine scaffold (Eli Lilly Co.; unpublished results) have shown that some elaborate alterations to MeNER, extra to hydroxylation, are tolerated for high affinity binding to NET. LY 2152041 is a potent ($\text{IC}_{50} = 10.8 \text{ nM}$) and selective NET inhibitor, which has been derived through hydroxylation and other structural modifications.

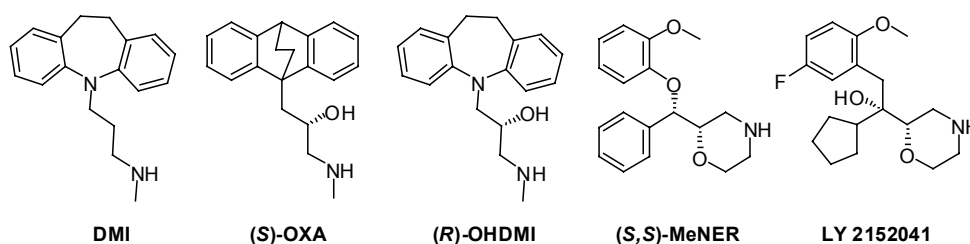
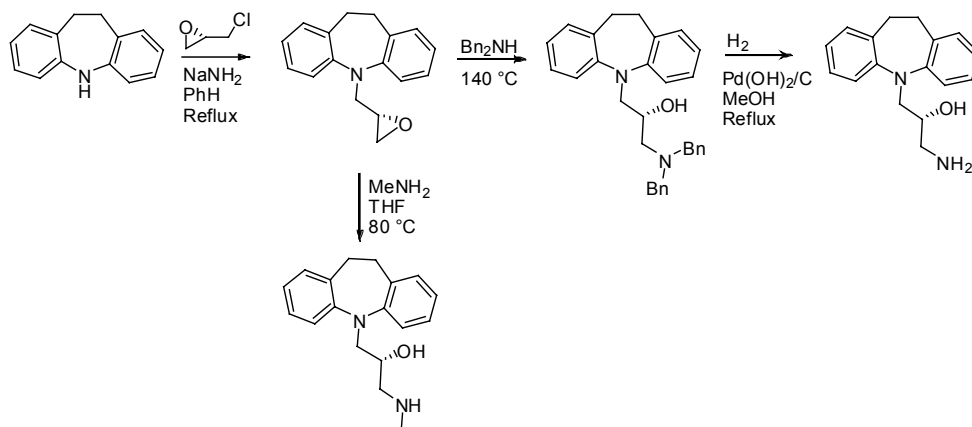


Figure 6. Structures of NET inhibitors derived from the DMI and aryloxymorpholine scaffold. Note that the spatial orientation of the hydroxyl groups in (*S*)-OXA and (*R*)-OHDMI are the same.

Chemistry and Pharmacology

The synthetic route used in the preparation of (*R*)-OHDMI and its primary amine precursor was similar to that used in the preparation of the *nor*-methyl precursor of DMI^{80,102,103} (Scheme 7). The key step in the synthesis was the formation of the homochiral epoxide **4**, which was subsequently aminated to yield (*R*)-OHDMI and its non-labelled precursor in 10 and 15% overall yield, respectively.



Scheme 7. Synthesis of (*R*)-OHDMI and its primary amine precursor.

Although the chemistry of racemic hydroxylated DMI derivatives has been previously described,^{102,103} no data on the potencies of such compounds had been reported. In an *in vitro* pharmacological assay, the potencies (K_i -values) of DMI, (*R*)-OHDMI, (*S,S*)-MeNER and LY 2152041 were 1.00, 8.29, 7.93 and 10.8 nM, respectively. The potencies of the new compounds were thus of the same order as (*S,S*)-MeNER, which merited radiolabelling and further evaluation by PET in non-human primates.

(*R*)-[*N*-methyl-¹¹C]OHDMI was obtained in a quantitative radiochemical yield from [¹¹C]methyl triflate without any added base or heating. The SR of (*R*)-[¹¹C]OHDMI was 390 GBq/μmol at time of injection into monkey and the product solution was chemically pure. [*O*-methyl-¹¹C]LY 2152041 was obtained quantitatively from [¹¹C]methyl iodide with a SR of 170 GBq/μmol (at time of injection). No competing *N*-alkylation was observed when this reaction was carried out under conditions similar to those used in the preparation of (*S,S*)-[¹¹C]MeNER.

PET in Non-Human Primates

Following injection of (*R*)-[¹¹C]OHDMI into a non-human primate, only 1.1% of the injected radioactivity entered brain, with a regional brain distribution in accordance with known densities of NETs. The maximum radioactivity level in brain after injection of (*R*)-[¹¹C]OHDMI was however too low for a useful PET radioligand.

In a PET measurement with [¹¹C]LY 2152041, radioactivity readily entered brain (3.9% I.D.) with accumulation in NET-rich regions as well as in the striatum. Because of the uptake in the striatum, cerebellum was used as a surrogate reference region. Cerebellum had earlier been shown to be almost devoid of uptake in PET measurements with (*S,S*)-[¹¹C]MeNER or (*S,S*)-[¹⁸F]FMeNER-D₂ and has been shown to be sparse in NET expression in rat, cat and human brain.^{23,25,74,79} Although using

cerebellum as a reference region, signal-to-noise ratios were lower than those obtained previously with (*S,S*)-[^{11}C]MeNER and (*S,S*)-[^{18}F]FMeNER-D₂.

Radiometabolite Analysis

There was very limited wash-out of radioactivity in any of the examined ROIs in the PET measurements with (*R*)-[^{11}C]OHDMI and [^{11}C]LY 2152041. An explanation for the low wash-out of radioactivity may be accumulation of a radiometabolite in brain. In accordance with this theory, lipophilic radiometabolites were observed in peripheral plasma after injection of both (*R*)-[^{11}C]OHDMI and [^{11}C]LY 2152041. In the case of (*R*)-[^{11}C]OHDMI, the radiometabolite had a retention time only 0.7 min shorter than parent. For [^{11}C]LY 2152041, the lipophilic radiometabolite was eluting at 7.5 min, 1.5 min after the parent compound, which indicates that the metabolite was more lipophilic than its mother radioligand. It is thus reasonable to assume that PET imaging may have been confounded by a radiometabolite.

(*R*)-[^{11}C]Thionisoxetine – a High Affinity NET Radioligand (Paper VI)

To visualize NET-poor regions such as cortex, which are of central interest in research on depression and ADHD,^{12,104} a more potent NET inhibitor than (*S,S*)-[^{18}F]FMeNER-D₂ is probably required. (*R*)-Thionisoxetine (Fig. 7, *vide infra*) is about three-fold more potent than (*R*)-nisoxetine,⁶² which had recently been labelled with ^{11}C and evaluated by Ding et al. in baboons.¹⁰⁵ In most reports, the racemate of nisoxetine has a reported affinity (IC_{50}) of 1.0 nM.^{22,25,72} In comparison, the IC_{50} of racemic MeNER is 2.5 nM.⁶³ Although these affinity values are not entirely comparable, they suggested that (*R*)-thionisoxetine is a more potent NET inhibitor than MeNER. Any increase in binding affinity, though modest, may be critical for imaging NETs with PET, since on theoretical grounds, binding potential (BP) is inversely proportional to binding affinity.

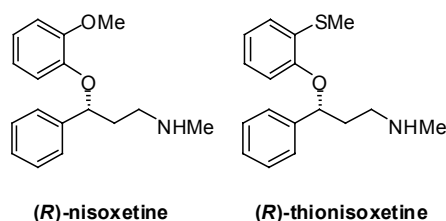


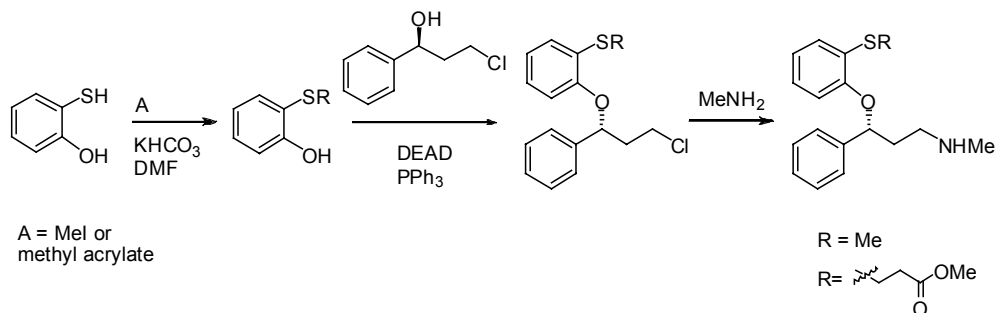
Figure 7. Structures of the (*R*)-enantiomers of nisoxetine and thionisoxetine.

Chemistry

The structure of (*R*)-thionisoxetine allows for radiolabelling at either the *S*-methyl or *N*-methyl moiety. We preferred a precursor that could be labelled by *S*-radiomethylation, since if the radioligand would show slow kinetics, we could radiolabel this moiety by ^{18}F -fluoromethylation. In previous reports it had been demonstrated that very few *N*-fluoromethyl compounds are stable enough to survive

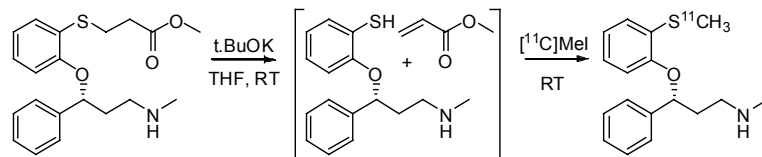
isolation,⁵¹ whereas *S*-[¹⁸F]fluoromethyl radioligands have been shown to be chemically stable, as exemplified by [¹⁸F]FMcN5652.⁹¹

Given the susceptibility of thiols to oxidize, we also aimed to prepare an *S*-protected precursor that might be stored and then deprotected *in situ* for radiomethylation with [¹¹C]methyl iodide.¹⁰⁶ Because of problems with preparing *S*-acetyl protected *o*-hydroxythiol,¹⁰⁷ we decided to protect the non-labelled precursor of (*R*)-thionisoxetine as an *S*- γ -propionic methyl ester.¹⁰⁸ Starting from *o*-hydroxythiophenol, (*R*)-thionisoxetine and its *S*- γ -propionic methyl ester precursor were obtained in 19 and 7% overall yield, respectively (Scheme 8).



Scheme 8. Synthesis of homochiral (*R*)-thionisoxetine and its γ -propionic methyl ester precursor.

In the radiolabelling of (*R*)-thionisoxetine, the thiol could be de-protected *in situ* under mild conditions using potassium *t*-butoxide in THF (Scheme 9). Radiomethylation under these conditions proceeded quantitatively from [¹¹C]methyl iodide at ambient temperature, yielding (*R*)-[¹¹C]thionisoxetine in a specific radioactivity of 304 GBq/ μ mol at the time of administration into cynomolgus monkey.



Scheme 9. Labelling of (*R*)-thionisoxetine in its *S*-methyl position with ¹¹C. The thiol precursor was generated *in situ* via a retro-Michael addition.

PET in Non-human Primate

After injection of (*R*)-[¹¹C]thionisoxetine into cynomolgus monkey, about 2.4% of the injected radioactivity entered brain with a regional distribution approximately matching that expected for NET. However, radioactivity also accumulated in striatum, an observation similar to those made in PET studies with [¹¹C]LY 2152041 and several other NET radioligands, including (*R*)-[¹¹C]nisoxetine.¹⁰⁵ As in the PET

study with [^{11}C]LY 2152041, we decided to use cerebellum as an alternative reference region. The maximum ratio of radioactivity in any ROI to the cerebellum in PET measurements with (*R*)-[^{11}C]thionisoxetine was no greater than 1.3. This ratio is lower than those observed with the NET radioligands, (*S,S*)-[^{11}C]MeNER and (*S,S*)-[^{18}F]FMeNER- D_2 . As in the case with [^{11}C]LY 2152041, this lower ratio, together with the accumulation of radioactivity in the striatum, severely limits the utility of (*R*)-[^{11}C]thionisoxetine as a PET radioligand for NET.

Since with (*R*)-[^{11}C]thionisoxetine there was no sign of wash-out of radioactivity from the striatum nor any sign that specific binding in thalamus increased with time, we expended no effort in preparing the ^{18}F -fluoromethyl analogue of this radioligand.

Analysis of Radiometabolites in Peripheral Monkey Plasma

Radioactivity in monkey plasma corresponding to (*R*)-[^{11}C]thionisoxetine decreased from 95% at 4 min to 53% at 45 min. One highly hydrophilic radiometabolite fraction represented the rest of the plasma radioactivity. In contrast to the PET study with [^{11}C]LY 2152041, in which about 10% of the radioactivity in monkey plasma was more lipophilic than parent at 4 min, we did not find support for radiometabolites entering brain and binding to the striatum in this case.

Present Status of Brain Imaging of NETs with PET

In the beginning of this project, a thorough investigation of the regional distribution of NETs in the primate brain had not been performed. We were thus largely relying on extrapolating data obtained from rodents to get an idea of the regional distribution and densities of NETs in the primate brain. This was accompanied with some uncertainty in radioligand development. Questions were raised about the density of NETs in the primate brain^{87,109} and the absence of NETs in striatum. Recently, however, *in vitro* studies have clarified the distribution and density of NETs in the primate brain.^{22,24}

The observed densities of NETs were roughly in accordance with the relative densities of NETs found in the rodent brain.²⁵ Thus, the highest levels of NETs were found in the LC and RN, followed by intermediate levels in the hypothalamus, thalamus and other brainstem regions. The lowest levels of NETs were found in the striatum and the molecular layer of cerebellum.²⁴ Although there was a high resemblance between rodents and primates in the expression of NETs, some important species differences were observed. In primates, the expression of NETs was about seven-, three- and five-fold lower in cortex, hypothalamus and thalamus relative to the LC. Furthermore, in a separate study, the B_{max} of NETs in human insular cortex homogenate was found to be 4.4 pmol/g tissue, which is roughly nine times less than in rodents.²²

These two studies are fundamentally very important. The regional distribution of NETs in the primate brain *in vitro* can be used to verify the distribution of NET radioligands *in vivo*. The density of NETs in primate brain can be applied for calculating affinity thresholds for future candidate NET radioligands.

During the last five years, about fifteen NET inhibitors have been evaluated as candidate NET radioligands in rodents and/or in primates. Nine of the candidates were evaluated within this project, whereas the rest were evaluated by the PET groups at Toronto,⁸⁷ Brookhaven^{86,105,110} and Emory^{83,111}. A number of these radioligands have shown accumulation of radioactivity in the striatum. In one case, this binding was ascribed to binding to DAT,¹¹² but in most cases this component of the binding in brain has remained uncharacterised and been regarded as non-specific.^{105,111} Within this thesis, two of the candidate radioligands, (*R*)-[¹¹C]thionisoxetine and [¹¹C]LY 2152041, showed such accumulation in the striatum. In the case with [¹¹C]LY 2152041, analysis of peripheral plasma implied that the component could be, at least partly, associated with a lipophilic radiometabolite. In the case with (*R*)-[¹¹C]thionisoxetine, no lipophilic radiometabolite was observed, which makes the binding harder to rationalise.

Logan has reasoned that this binding, similarly to the binding of [³H]DMI *in vitro*, is of low affinity and to a second non-adrenergic site.¹¹³ However, in the *in vitro* studies with [³H]DMI, this binding could be inhibited by the inclusion of a high concentration of NET inhibitor,⁷⁸ whereas the binding of (*R*)-[¹¹C]nisoxetine in striatum was unaffected in a pre-treatment experiment with nisoxetine (1 mg/kg) *in vivo*. Furthermore, the binding of [³H]nisoxetine to human cortical homogenate *in vitro* was found to represent a single class of binding sites,²² which contradicts Logan's hypothesis. Although the low-affinity binding of [³H]DMI was shown to be sensitive to incubation conditions,^{114,115} which may not be altered *in vivo*, the cause of the contrasting results obtained with [³H]nisoxetine *in vitro* and [¹¹C]nisoxetine *in vivo* is more likely to reflect a BBB permeable radiometabolite rather than binding to a second site with low affinity. This implies that a more detailed radiometabolite analysis may be warranted for new (and old) NET radioligands.

The most promising NET radioligands evaluated so far are the aryloxy morpholine derivatives, (*S,S*)-[¹¹C]MeNER and (*S,S*)-[¹⁸F]FMeNER-D₂. It has been argued that (*S,S*)-[¹¹C]MeNER, although it has slow kinetics, is suitable for PET imaging of NETs in man.¹¹³ Recently however, the test-retest variabilities in BPs when using (*S,S*)-[¹¹C]MeNER were found to be too large (17 to 31%) to reliably assess NET density. In addition, the binding of (*S,S*)-[¹¹C]MeNER was not found to be saturable at supra-therapeutic doses, a finding that was also supported by the PET group at Johns Hopkins.¹¹⁶ Although NET can be imaged with (*S,S*)-[¹¹C]MeNER, its disadvantages are such that it is not useful in clinical research. As this thesis is being written, clinical studies with (*S,S*)-[¹⁸F]FMeNER-D₂ are carried out. Some promising human *in vitro* imaging data were reported within this thesis. In addition, a recent occupancy study with atomoxetine and (*S,S*)-[¹⁸F]FMeNER-D₂ in monkeys demonstrated a saturable and dose-dependent accumulation in the LC.¹¹⁶ This was never observed in the clinical occupancy studies with (*S,S*)-[¹¹C]MeNER^{90,117} nor in occupancy studies with cocaine and (*S,S*)-[¹¹C]MeNER in baboons.¹¹³ Thus, (*S,S*)-[¹⁸F]FMeNER-D₂ clearly represents the most promising imaging agent for central NETs in the human brain reported to date.

Challenges in Future NET Radioligand Development

The challenges in further NET radioligand development are similar to those faced in the development of radioligands for other receptor or transporter systems. However, there are some difficulties in NET radioligand development that are specific for NET. These are listed below:

- i) The expression of NETs in the human brain is low; only 4.4 pmol/mg NET is present in the insular cortex. In comparison, the density of DATs in putamen is 212 pmol/g wet tissue¹¹⁸ and the corresponding density of SERTs is 143 pmol/g protein in prefrontal cortex.¹¹⁹ Although this comparison is not entirely fair, because the compared regions are not the regions of highest density for the given transporters (except DAT), it gives an idea about the relationship between the monoamine transporter concentrations *in vivo*. The lower density of NETs requires that a suitable radioligand would need higher affinity than those presently used for DAT¹²⁰ or SERT¹²¹ imaging. In human insular cortex, the affinity of an efficient radioligand should be at least 0.9 nM.
- ii) Not only is the expression of NETs low in brain, the highest levels of NET expression in the primate brain are localized within small brain regions, like LC and RN, which are challenging to image with PET. It is estimated that the number of neurons in the LC, which is the most dense NET-region in primate brain, is only of the order of 40,000 to 50,000.¹²² In addition, the size of this region is just a few millimetres.
- iii) The lack of potent and selective NET platforms suitable for NET imaging. Candidate radioligands from all known potent and selective NET platforms have been evaluated as candidate NET radioligands. Only one “hit” was found during this screening process, namely (*S,S*)-MeNER, which is based on the reboxetine platform. Further development of this scaffold resulted in (*S,S*)-FMeNER-D₂, LY 2152041 and an iodinated analogue, (*S,S*)-INER,¹²³ that were about equipotent to (*S,S*)-MeNER. Based on SAR on the related nisooxetine platform, it is uncertain if any more potent NET inhibitors will be obtained from the reboxetine scaffold. Further NET radioligand development may require extensive synthesis and SAR analysis of new compounds.

CONCLUSIONS

A series of candidate NET radioligands were prepared and evaluated by PET in cynomolgus monkey *in vivo*. Most of the candidates had been developed in the pharmaceutical industry before this project started, but had not been evaluated as candidate NET radioligands. During this process some improvements were made in the ^{18}F -labelling of aryl fluoromethyl ethers and sulfides. Three new NET inhibitors were developed, (*S,S*)-FMeNER-D₂, (*R*)-OHDMI and LY 2152041, each was found to be a potent NET inhibitor. Two of the candidates, (*S,S*)-[^{11}C]MeNER and (*S,S*)-[^{18}F]FMeNER-D₂, were found to successfully image NETs in preliminary PET measurements in cynomolgus monkey as well as in *post mortem* human brain autoradiography. (*S,S*)-[^{18}F]FMeNER-D₂ has the potential to be the first radioligand useful for quantitative imaging of NETs in the human brain *in vivo*.

REFERENCES

1. Tellioglu T, Robertson R. Genetic or acquired deficits in the norepinephrine transporter: current understanding of clinical implications. *Exp. Rev. Mol. Med.* 2001;<http://www-ermm.cbcu.cam.ac.uk/01003878h.htm>.
2. Blakely R, De Felice R, Hartzell H. Molecular physiology of norepinephrine and serotonin transporters. *J Exp Biol* 1994;**196**:263-281.
3. Sullivan GM, Coplan JD, Kent JM, Gorman JM. The noradrenergic system in pathological anxiety: a focus on panic with relevance to generalized anxiety and phobias. *Biol Psychiatry* 1999;**46**(9):1205-18.
4. Spencer T, Heiligenstein J, Biederman J, Faries D, Kratochvil C, Conners C, Potter W. Results from 2 proof-of-concept, placebo-controlled studies of atomoxetine in children with attention-deficit/hyperactivity disorder. *J Clin Psychiatry* 2002;**63**(12):1140-7.
5. Klimek V, Stockmeier C, Overholser J, Meltzer HY, Kalka S, Dilley G, Ordway GA. Reduced levels of norepinephrine transporters in the locus coeruleus in major depression. *J Neurosci* 1997;**17**(21):8451-8.
6. Brunello N, Mendlewicz J, Kasper S, Leonard B, Montgomery S, Nelson J, Paykel E, Versiani M, Racagni G. The role of noradrenaline and selective noradrenaline reuptake inhibition in depression. *Eur Neuropsychopharmacol* 2002;**12**(5):461-75.
7. Macey DJ, Smith HR, Nader MA, Porrino LJ. Chronic cocaine self-administration upregulates the norepinephrine transporter and alters functional activity in the bed nucleus of the stria terminalis of the rhesus monkey. *J Neurosci* 2003;**23**(1):12-6.
8. Tejani-Butt S, Yang J, Zaffar H. Norepinephrine transporter sites are decreased in the locus coeruleus in Alzheimer's disease. *Brain Research* 1993;**631**(1):147-50.
9. Kuhn R. Treatment of depressive states with an iminodibenzyl derivative (G 22355). *Schweiz Med Wochenschr* 1957;**87**(35-36):1135-40.
10. Loomer HP, Saunders JC, Kline NS. A clinical and pharmacodynamic evaluation of iproniazid as a psychic energizer. *Psychiatr Res Rep Am Psychiatr Assoc* 1957;**135**(8):129-41.
11. Bymaster FP, Beedle EE, Findlay J, Gallagher PT, Krushinski JH, Mitchell S, Robertson DW, Thompson DC, Wallace L, Wong DT. Duloxetine (Cymbalta), a dual inhibitor of serotonin and norepinephrine reuptake. *Bioorg Med Chem Lett* 2003;**13**(24):4477-80.
12. Bymaster FP, Katner JS, Nelson DL, Hemrick-Luecke SK, Threlkeld PG, Heiligenstein JH, Morin SM, Gehlert DR, Perry KW. Atomoxetine increases extracellular levels of norepinephrine and dopamine in prefrontal cortex of rat: a potential mechanism for efficacy in attention deficit/hyperactivity disorder. *Neuropsychopharmacology* 2002;**27**(5):699-711.

13. Sesack SR, Hawrylak VA, Matus C, Guido MA, Levey AI. Dopamine axon varicosities in the prelimbic division of the rat prefrontal cortex exhibit sparse immunoreactivity for the dopamine transporter. *J Neurosci* 1998;**18**(7):2697-708.
14. Paczkowski FA, Bryan-Lluka LJ, Porzgen P, Bruss M, Bonisch H. Comparison of the pharmacological properties of cloned rat, human, and bovine norepinephrine transporters. *J Pharmacol Exp Ther* 1999;**290**(2):761-7.
15. Phelps ME. PET: the merging of biology and imaging into molecular imaging. *J Nucl Med* 2000;**41**(4):661-81.
16. Farde L, Hall H, Ehrin E, Sedvall G. Quantitative analysis of D2 dopamine receptor binding in the living human brain by PET. *Science* 1986;**231**(4735):258-61.
17. Farde L, Nordstrom AL, Wiesel FA, Pauli S, Halldin C, Sedvall G. Positron emission tomographic analysis of central D1 and D2 dopamine receptor occupancy in patients treated with classical neuroleptics and clozapine. Relation to extrapyramidal side effects. *Arch Gen Psychiatry* 1992;**49**(7):538-44.
18. Lingford-Hughes A, Wilson SJ, Feeney A, Grasby PG, Nutt DJ. A proof-of-concept study using [¹¹C]flumazenil PET to demonstrate that pagoclone is a partial agonist. *Psychopharmacology (Berl)* 2005;**180**(4):789-91.
19. Bergstrom M, Grahnen A, Langstrom B. Positron emission tomography microdosing: a new concept with application in tracer and early clinical drug development. *Eur J Clin Pharmacol* 2003;**59**(5-6):357-66.
20. Holford N. Concepts and usefulness of pharmacokinetic-pharmacodynamic modelling. *Fundam Clin Pharmacol* 1990;**4**(Suppl 2):93s-101s.
21. Halldin C, Gulyas B, Farde L. PET studies with carbon-11 radioligands in neuropsychopharmacological drug development. *Curr Pharm Des* 2002;**7**:1907-1929.
22. Mash DC, Ouyang Q, Qin Y, Pablo J. Norepinephrine transporter immunoblotting and radioligand binding in cocaine abusers. *J Neurosci Methods* 2005;**143**(1):79-85.
23. Donnan G, Kaczmarczyk S, Paxinos G, Chilco P, Kalnins R, Woodhouse D, Mendelsohn F. Distribution of catecholaminergic uptake sites in human brain as determined by quantitative [³H]mazindol autoradiography. *J Comp Neurol* 1991;**304**:419-434.
24. Smith HR, Beveridge TJ, Porrino LJ. Distribution of norepinephrine transporters in the non-human primate brain. *Neuroscience* 2006;**138**(2):703-14.
25. Tejani-Butt S. [³H]Nisoxetine: A radioligand for quantitation of norepinephrine uptake sites by autoradiography or by homogenate binding. *J Pharm Exp Ther* 1992;**260**:427-436.
26. Halldin C, Farde L, Hogberg T, Mohell N, Hall H, Suhara T, Karlsson P, Nakashima Y, Swahn CG. Carbon-11-FLB 457: a radioligand for extrastriatal D2 dopamine receptors. *J Nucl Med* 1995;**36**(7):1275-81.

27. Fowler JS, Volkow ND, Wang GJ, Gatley SJ, Logan J. [(11)]Cocaine: PET studies of cocaine pharmacokinetics, dopamine transporter availability and dopamine transporter occupancy. *Nucl Med Biol* 2001;**28**(5):561-72.
28. Bock N, Quentin DJ, Huther G, Moll GH, Banaschewski T, Rothenberger A. Very early treatment with fluoxetine and reboxetine causing long-lasting change of the serotonin but not the noradrenaline transporter in the frontal cortex of rats. *World J Biol Psychiatry* 2005;**6**(2):107-12.
29. Kretzschmar M, Brust P, Zessin J, Cumming P, Bergmann R, Johannsen B. Autoradiographic imaging of the serotonin transporter in the brain of rats and pigs using S-([¹⁸F]fluoromethyl)-(+)-McN5652. *Eur Neuropsychopharmacol* 2003;**13**(5):387-97.
30. Halldin C, Swahn C-G, Farde L, Sedvall G. Radioligand disposition and metabolism: Kluwer Academic Publishers, 1995.
31. Hume SP, Hirani E, Opacka-Juffry J, Osman S, Myers R, Gunn RN, McCarron JA, Clark RD, Melichar J, Nutt DJ, Pike VW. Evaluation of [O-methyl-¹¹C]RS-15385-197 as a positron emission tomography radioligand for central alpha2-adrenoceptors. *Eur J Nucl Med* 2000;**27**(5):475-84.
32. Osman S, Lundkvist C, Pike VW, Halldin C, McCarron JA, Swahn CG, Farde L, Ginovart N, Luthra SK, Gunn RN, Bench CJ, Sargent PA, Grasby PM. Characterisation of the appearance of radioactive metabolites in monkey and human plasma from the 5-HT1A receptor radioligand, [carbonyl-¹¹C]WAY-100635--explanation of high signal contrast in PET and an aid to biomathematical modelling. *Nucl Med Biol* 1998;**25**(3):215-23.
33. Balle T, Halldin C, Andersen L, Hjorth Alifrangis L, Badolo L, Gjervig Jensen K, Chou YW, Andersen K, Perregaard J, Farde L. New α_1 -adrenoceptor antagonists derived from the antipsychotic sertindole - carbon-11 labelling and pet examination of brain uptake in the cynomolgus monkey. *Nucl Med Biol* 2004;**31**(3):327-36.
34. Lipinski CA, Lombardo F, Dominy BW, Feeney PJ. Experimental and computational approaches to estimate solubility and permeability in drug discovery and development settings. *Adv Drug Deliv Rev* 2001;**46**(1-3):3-26.
35. Waterhouse RN. Determination of lipophilicity and its use as a predictor of blood-brain barrier penetration of molecular imaging agents. *Mol Imaging Biol* 2003;**5**(6):376-89.
36. Welch MJ, Chi DY, Mathis CJ, Kilbourn MR, Brodack JW, Katzenellenbogen JA. Biodistribution of N-alkyl and N-fluoroalkyl derivatives of spiroperidol; radiopharmaceuticals for PET studies of dopamine receptors. *Int J Rad Appl Instrum B* 1986;**13**(5):523-6.
37. Zoghbi SS, Shetty HU, Ichise M, Fujita M, Imaizumi M, Liow JS, Shah J, Musachio JL, Pike VW, Innis RB. PET imaging of the dopamine transporter with ¹⁸F-FECNT: a polar radiometabolite confounds brain radioligand measurements. *J Nucl Med* 2006;**47**(3):520-7.

38. Någren K, Truong P, Helin S, Amir A, Halldin C. Experience from two systems for recirculation production of [^{11}C]methyl iodide produced from target produced [^{11}C]methane. *J Label Compd Radiopharm* 2003;**46**:S76.
39. Någren K, Muller L, Halldin C, Swahn CG, Lehtikainen P. Improved synthesis of some commonly used PET radioligands by the use of [^{11}C]methyl triflate. *Nucl Med Biol* 1995;**22**(2):235-239.
40. Ishiwata K, Ishii SI, Shinoda M, Maekawa S, Senda M. Automated synthesis of radiochemically pure ^{11}C labelled ethyl, propyl and butyl iodides. *Appl Radiat Isot* 1999;**50**(4):693-697.
41. Rahman O, Kihlberg T, Langstrom B. Aryl triflates and [^{11}C]/[^{13}C]carbon monoxide in the synthesis of $^{11}\text{C}/^{13}\text{C}$ -amides. *J Org Chem* 2003;**68**(9):3558-62.
42. Finn RD, Christman DR, Ache HJ, Wolf AP. The preparation of ^{11}C -cyanide for use in the synthesis of organic radiopharmaceuticals II. *Int J Appl Radiat Isot* 1971;**22**(12):735-44.
43. Luthra SK, Pike VW, Brady F. Preparation of Some n.c.a. 1- ^{11}C acid chlorides as labelling agents. *Appl Radiat Isot* 1990;**41**(5):471-476.
44. Oh SJ, Chi DY, Mosdzianowski C, Kim JY, Gil HS, Kang SH, Ryu JS, Moon DH. Fully automated synthesis of ^{18}F fluoromisonidazole using a conventional ^{18}F -FDG module. *Nucl Med Biol* 2005;**32**(8):899-905.
45. Bergman J, Eskola O, Lehtikainen P, Solin O. Automated synthesis and purification of ^{18}F -bromofluoromethane at high specific radioactivity. *Appl Radiat Isot* 2001;**54**(6):927-933.
46. Iwata R, Pascali C, Bogner A, Furumoto S, Terasaki K, Yanai K. [^{18}F]Fluoromethyl triflate, a novel and reactive [^{18}F]fluoromethylating agent: preparation and application to the on-column preparation of [^{18}F]fluorocholine. *Appl Radiat Isot* 2002;**57**:347-352.
47. Coenen HH, Colosimo M, Schuller M, Stocklin G. Preparation of n.c.a. ^{18}F - CH_2BrF via aminopolyether supported nucleophilic substitution. *J Label Compd Radiopharm* 1986;**23**(6):587-595.
48. Block D, Coenen HH, Stocklin G. The n.c.a. nucleophilic ^{18}F -fluorination of 1,*N*-disubstituted alkanes as fluoroalkylation agents. *J Label Compd Radiopharm* 1987;**24**(9):1029-1042.
49. Neal TR, Apana S, Berridge MS. Improved synthesis of [^{18}F]fluoromethyl tosylate, a convenient reagent for radiofluoromethylations. *J Label Compd Radiopharm* 2005;**48**(8):557-568.
50. Zheng L, Berridge MS. Synthesis of ^{18}F -fluoromethyl iodide, a synthetic precursor for fluoromethylation of radiopharmaceuticals. *Appl Radiat Isot* 2000;**52**(1):55-61.
51. Zhang MR, Ogawa M, Furutsuka K, Yoshida Y, Suzuki K. ^{18}F -Fluoromethyl iodide (^{18}F -FCH₂I) preparation and reactions with phenol, thiophenol, amide and amine functional groups. *J Fluorine Chem* 2004;**125**(12):1879-1886.
52. Bergman J, Solin O. Fluorine-18-labeled fluorine gas for synthesis of tracer molecules. *Nucl Med Biol* 1997;**24**(7):677-83.

53. Olsson H, Halldin C, Farde L. Differentiation of extrastriatal dopamine D2 receptor density and affinity in the human brain using PET. *Neuroimage* 2004;**22**(2):794-803.
54. Hall H, Halldin C, Farde L, Sedvall G. Whole hemisphere autoradiography of the postmortem human brain. *Nucl Med Biol* 1998;**25**:715-719.
55. Hall H, Hurd Y, Pauli S, Halldin C, Sedvall G. Human Brain Imaging Post-mortem - Whole Hemisphere Technologies. *Int Rev Psych Res Meth Biol Psych* 2001(Special Issue 13):12-17.
56. Farde L, Eriksson L, Blomquist G, Halldin C. Kinetic analysis of central [¹¹C]raclopride binding to D2-dopamine receptors studied by PET-a comparison to the equilibrium analysis. *J Cereb Blood Flow Metab* 1989;**9**(5):696-708.
57. Olsson H, Farde L. Potentials and pitfalls using high affinity radioligands in PET and SPET determinations on regional drug induced D2 receptor occupancy-a simulation study based on experimental data. *Neuroimage* 2001;**14**(4):936-45.
58. Ghose S, Fujita M, Morrison P, Uhl G, Murphy DL, Mozley PD, Schou M, Halldin C, Innis R. Specific in vitro binding of (S,S)-[³H]MeNER to norepinephrine transporters. *Synapse* 2005;**56**(2):100-4.
59. Henze E, Huang SC, Ratib O, Hoffman E, Phelps ME, Schelbert HR. Measurements of regional tissue and blood-pool radiotracer concentrations from serial tomographic images of the heart. *J Nucl Med* 1983;**24**(11):987-96.
60. Javaid JI, Perel JM, Davis JM. Inhibition of biogenic amines uptake by imipramine, desipramine, 2 OH-imipramine and 2 OH-desipramine in rat brain. *Life Sci* 1979;**24**(1):21-8.
61. Waldmeier PC, Baumann PA, Hauser K, Maitre L, Storni A. Oxaprotiline, a noradrenaline uptake inhibitor with an active and an inactive enantiomer. *Biochem Pharmacol* 1982;**31**(12):2169-76.
62. Gehlert DR, Hemrick-Luecke SK, Schober DA, Krushinski J, Howbert JJ, Robertson DW, Wong DT, Fuller RW. (R)-thionisoxetine, a potent and selective inhibitor of central and peripheral norepinephrine uptake. *Life Sci* 1995;**56**(22):1915-20.
63. Melloni P, Carniel G, Della Torre A, Bonsignori A, Buonamici M, Pozzi O, Ricciardi S, Rossi A. Potential antidepressant agents. α -Aryloxy-benzyl derivatives of ethanolamine and morpholine. *Eur J Med Chem Chim Ther* 1984;**19**:235-242.
64. Chumpradit S, Kung M, Panyachotipun C, Prapansiri V, Foulun C, Brooks B, Szabo S, Tejani-Butt S, Frazer A, Kung H. Iodinated tomoxetine derivatives as selective ligands for serotonin and norepinephrine uptake sites. *J Med Chem* 1992;**35**:4492-4497.
65. Wong DT, Threlkeld PG, Best KL, Bymaster FP. A new inhibitor of norepinephrine uptake devoid of affinity for receptors in rat brain. *J Pharmacol Exp Ther* 1982;**222**:61.

66. Bøgesø KP, Christiansen A, Hyttel J, Liljefors T. 3-Phenyl-1-Indanamines. Potential antidepressant activity and potent inhibitors of dopamine, norepinephrine and serotonin uptake. *J Med Chem* 1985;**28**:1817-1828.
67. Blough BE, Holmquist CR, Abraham P, Kuhar MJ, Carroll FI. 3 α -(4-Substituted phenyl)nortropane-2 β -carboxylic acid methyl esters show selective binding at the norepinephrine transporter. *Bioorg Med Chem Lett* 2000;**10**(21):2445-7.
68. Hoepping A, Johnson KM, George C, Flippen-Anderson J, Kozikowski AP. Novel conformationally constrained tropane analogues by 6-endo-trig radical cyclization and stille coupling - switch of activity toward the serotonin and/or norepinephrine transporter. *J Med Chem* 2000;**43**(10):2064-71.
69. Maryanoff B, McComsey D, Gardocki J, Shank R, Costanzo M, Nortey S, Schneider C, Setler P. Pyrroloisoquinoline antidepressants 2. In-depth exploration of structure-activity relationships. *J Med Chem* 1987;**30**:1433-1454.
70. Hyttel J. Citalopram - pharmacological profile of a specific serotonin uptake inhibitor with antidepressant activity. *Prog Neuro-Psychopharmacol & Biol Psychiat* 1982;**6**:277-295.
71. Gehlert D, Schober D, Hemrick-Luecke S, Krushinski J, Howbert J, Robertson D, Fuller R, Wong D. Novel halogenated analogs of tomoxetine that are potent and selective inhibitors of norepinephrine uptake in brain. *Neurochem Int* 1995;**26**:47-52.
72. Haka M, Kilbourn M. Synthesis and regional mouse brain distribution of [¹¹C]nisoxetine, a norepinephrine transporter inhibitor. *Nucl Med Biol* 1989;**16**:771-774.
73. Ordway G, Stockmeier C, Cason G, Klimek V. Pharmacology and distribution of norepinephrine transporters in the human locus coeruleus and raphe nuclei. *J Neurosci.* 1997;**17**(5):1710-1719.
74. Charnay Y, Leger L, Vallet P, HOF P, Juovet M, Bouras C. [³H]Nisoxetine binding sites in the cat brain: an autoradiographic study. *Neuroscience* 1995;**69**:259-270.
75. Zavidovskaia GI. The use of LU-3-010 in the treatment of depressive states. *Zh Nevropatol Psikhiatr Im S S Korsakova* 1969;**69**(4):594-8.
76. Stromgren LS, Friderichsen T. Lu 5-003 in antidepressive therapy. *Nord Psykiatr Tidsskr* 1971;**25**(2):119-28.
77. Cusack B, Nelson A, Richelson E. Binding of antidepressants to human brain receptors: focus on newer generation compounds. *Psychopharmacol* 1994;**114**(4):559-65.
78. Bäckström IT, Marcusson JO. High- and low-affinity [³H]desipramine-binding sites in human postmortem brain tissue. *Neuropsychobiol* 1990;**23**(2):68-73.
79. Gross-Isseroff R, Israeli M, Biegon A. Autoradiographic analysis of [³H]desmethylinipramine binding in the human brain postmortem. *Brain Res* 1988;**456**(1):120-6.

80. Van Dort M, Kim J, Tluczek L, Wieland D. Synthesis of ^{11}C -labeled desipramine and its metabolite 2-hydroxydesipramine: potential radiotracers for PET studies of the norepinephrine transporter. *Nucl Med Biol* 1997;**24**:707-711.
81. Nagren K, Halldin C, Muller L, Swahn CG, Lehtikainen P. Comparison of ^{11}C methyl triflate and [^{11}C]methyl iodide in the synthesis of PET radioligands such as [^{11}C]β-CIT and [^{11}C]β-CFT. *Nucl Med Biol* 1995;**22**(8):965-970.
82. Sandell J, Langer O, Larsen P, Dolle F, Vaufrey F, Demphel S, Crouzel C, Halldin C. Improved specific radioactivity of the PET radioligand [^{11}C]FLB 457 by use of the GE medical systems PETtrace MeI MicroLab. *J Labelled Compd Radiopharm* 2000;**43**:331-338.
83. McConathy J, Owens MJ, Kilts CD, Malveaux EJ, Camp VM, Votaw JR, Nemeroff CB, Goodman MM. Synthesis and biological evaluation of [^{11}C]talopram and [^{11}C]talsupram: candidate PET ligands for the norepinephrine transporter. *Nucl Med Biol* 2004;**31**(6):705-18.
84. Wong E, Sonders M, Amara S, Tinholt P, Piercey M, Hoffmann W, Hyslop D, Franklin S, Porsolt R, Bonsignori A, Carfagna N, McArthur N. Reboxetine: a pharmacologically potent, selective, and specific norepinephrine reuptake inhibitor. *Biol Psychiatry* 2000;**47**:818-29.
85. Öhman D, Norlander B, Peterson C, Bengtsson F. Bioanalysis of racemic reboxetine and its desethylated metabolite in a therapeutic drug monitoring setting using solid phase extraction and HPLC. *Ther Drug Monit* 2001;**23**:27-34.
86. Ding YS, Lin KS, Garza V, Carter P, Alexoff D, Logan J, Shea C, Xu Y, King P. Evaluation of a new norepinephrine transporter PET ligand in baboons, both in brain and peripheral organs. *Synapse* 2003;**50**(4):345-52.
87. Wilson A, Johnson D, Mozley P, Hussey D, Ginovart N, Nobrega J, Garcia A, Meyer J, Houle S. Synthesis and in vivo evaluation of novel radiotracers for the in vivo imaging of the norepinephrine transporter. *Nucl Med Biol* 2003;**30**(2):85-92.
88. Murray M, Field SL. Inhibition and metabolite complexation of rat hepatic microsomal cytochrome P450 by tricyclic antidepressants. *Biochem Pharmacol* 1992;**43**(10):2065-71.
89. Dostert P, Benedetti MS, Poggesi I. Review of the pharmacokinetics and metabolism of reboxetine, a selective noradrenaline reuptake inhibitor. *Eur Neuropsychopharmacol* 1997;**7 Suppl 1**:S23-35; discussion S71-3.
90. Andrée B, Schou M, Mozley PD, Vandenhende ZFR, Farde L, Halldin C. Test-retest evaluation of central [^{11}C]MeNER binding to the norepinephrine transporter in healthy subjects using PET. *manuscript* 2006.
91. Marjamäki P, Zessin J, Eskola O, Gronroos T, Haaparanta M, Bergman J, Lehtikainen P, Forsback S, Brust P, Steinbach J, Solin O. *S*-[^{18}F]fluoromethyl-(+)-McN5652, a PET tracer for the serotonin transporter: evaluation in rats. *Synapse* 2003;**47**(1):45-53.

-
92. Hwang DR, Jerabek PA, Kadmon D, Kilbourn MR, Patrick TB, Welch MJ. 2-^[18F]fluoroputrescine: preparation, biodistribution, and mechanism of defluorination. *Int J Rad Appl Instrum [A]* 1986;**37**(7):607-12.
93. Hamill T, Burns H, Eng W, Ryan C, Krause S, Gibson R, Hargreaves R. An improved fluorine-18 labeled neurokinin-1 receptor ligand. *Mol Imaging Biol* 2002;**4**(4, Suppl. 1):S34.
94. Fowler J, Wang G, Logan J, Xie S, Volkow N, MacGregor R, Schlyer D, Pappas N, Alexoff D, Patlak C. Selective reduction of radiotracer trapping by deuterium substitution: comparison of carbon-11-L-deprenyl and carbon-11-deprenyl-D2 for MAO B mapping. *J Nucl Med*. 1995;**36**(7):1255-62.
95. Page G, Chalon S, Emond P, Maloteaux JM, Hermans E. Pharmacological characterisation of (E)-N-(3-iodoprop-2-enyl)-2 β -carbomethoxy-3 β -(4'-methylphenyl)nortropane (PE2I) binding to the rat neuronal dopamine transporter expressed in COS cells. *Neurochem Int* 2002;**40**(2):105-13.
96. Suzuki M, Yamaguchi K, Honda G, Iwata R, Furumoto S, Jeong MG, Fukuda H, Itoh M. An experimental study on O-^{18F} fluoromethyl-L-tyrosine for differentiation between tumor and inflammatory tissues. *Annals of Nuclear Medicine* 2005;**19**(7):589-595.
97. Hargreaves R. Imaging substance P receptors (NK1) in the living human brain using positron emission tomography. *J Clin Psychiatry* 2002;**63** Suppl 11:18-24.
98. Heiss WD, Habedank B, Klein JC, Herholz K, Wienhard K, Lenox M, Nutt R. Metabolic rates in small brain nuclei determined by high-resolution PET. *J Nucl Med* 2004;**45**(11):1811-5.
99. Chin FT, Morse CL, Shetty HU, Pike VW. Automated radiosynthesis of F-18 SPA-RQ for imaging human brain NK1 receptors with PET. *J Label Compd Radiopharm* 2006;**49**(1):17-31.
100. Antonsen Ø, Benneche T, Undheim K. Syntheses of sulfinylmethyl ethers and conversion of these into halomethyl and acyloxymethyl ethers. *Acta Chem Scand Ser B* 1988;**42**:515-523.
101. Paul T, Ingold KU. A method for thermal generation of aryloxyl radicals at ambient temperatures: application to low-density lipoprotein (LDL) oxidation. *Angew Chem Int Ed Engl* 2002;**41**(5):804-6.
102. Schindler W, Hafliger F. Über derivaten des Iminodibenzyls. *Helv Chim Acta* 1954;**59**:472.
103. Levy O, Erez M, Varon D, Keinan E. A new class of antiarrhythmic-defibrillatory agents. *Bioorg Med Chem Lett* 2001;**11**(22):2921-6.
104. Sheline YI. Neuroimaging studies of mood disorder effects on the brain. *Biol Psychiatry* 2003;**54**(3):338-52.
105. Ding YS, Lin KS, Logan J, Benveniste H, Carter P. Comparative evaluation of positron emission tomography radiotracers for imaging the norepinephrine transporter: (S,S) and (R,R) enantiomers of reboxetine analogs ([¹¹C]methylreboxetine, 3-Cl-[¹¹C]methylreboxetine and

- [¹⁸F]fluororeboxetine), (R)-[¹¹C]nisoxetine, [¹¹C]oxaprotiline and [¹¹C]lortalamine. *J Neurochem* 2005;**94**(2):337-51.
106. Zessin J, Gucker P, Ametamey SM, Steinbach J, Brust P, Vollenweider FX, Johannsen B, Schubiger PA. Efficient synthesis of enantiomerically pure thioester precursors of [¹¹C]McN-5652 from racemic McN-5652. *J Label Compd Radiopharm* 1999;**42**:1301-1312.
107. McKinnon DM. Acyl transfer in o-hydroxybenzenethiol. *Can J Chem* 1980;**58**:2761-2764.
108. Becht J-M, Wagner A, Mioskowski C. Facile introduction of SH group on aromatic substrates via electrophilic substitution reactions. *J Org Chem* 2003;**68**:5758-5761.
109. Kung MP, Choi SR, Hou C, Zhuang ZP, Foulon C, Kung HF. Selective binding of 2-[¹²⁵I]iodo-nisoxetine to norepinephrine transporters in the brain. *Nucl Med Biol* 2004;**31**(5):533-41.
110. Lin K-S, Ding Y-S, Betzel T, Quandt G. Synthesis and in vivo evaluation of ¹¹C labeled mazindol analogs for imaging the norepinephrine transporter with PET. *J Label Compd. Radiopharm* 2005;**48**:S152.
111. McConathy J, Owens MJ, Kilts CD, Malveaux EJ, Votaw JR, Nemeroff CB, Goodman MM. Synthesis and biological evaluation of trans-3-phenyl-1-indanamines as potential norepinephrine transporter imaging agents. *Nucl Med Biol* 2005;**32**(6):593-605.
112. Musachio JL, Hong J, Ichise M, Seneca N, Brown AK, Liow J-S, Halldin C, Innis RB, Pike VW, He R, Zhou J, Kozikowski AP. Development of new brain imaging agents based upon cocaine-modafinil hybrid monoamine transporter inhibitors. *Bioorg Med Chem Lett* 2006;in press.
113. Logan J, Ding YS, Lin KS, Pareto D, Fowler J, Biegon A. Modeling and analysis of PET studies with norepinephrine transporter ligands: the search for a reference region. *Nucl Med Biol* 2005;**32**(5):531-42.
114. Biegon A, Rainbow TC. Localization and characterization of [³H]desmethylinipramine binding sites in rat brain by quantitative autoradiography. *J Neurosci* 1983;**3**(5):1069-76.
115. Lee CM, Javitch JA, Snyder SH. Characterization of [³H]desipramine binding associated with neuronal norepinephrine uptake sites in rat brain membranes. *J Neurosci* 1982;**2**(10):1515-25.
116. Seneca N, Gulyás B, Varrone A, Schou M, Tauscher J, Vandenhende F, Kielbasa W, Farde L, Innis RB, Halldin C Atomoxetine occupies the norepinephrine transporter in a dose-dependent fashion: A PET study in nonhuman primate brain using (S,S)-[¹⁸F]FMeNER-D₂ *manuscript*
117. Wong D, Kuwabara H, Mozley P, Dannals R, Kumar A, Ye W, Brasic J, Alexander M, Mathews W, Holt D, Vandenhende F, A G. Characterization of dose dependent norepinephrine transporter blockade by atomoxetine in human brain using [¹¹C]MeNER PET. *Brain and Brain PET* 2005 2005:BP-12.

118. Madras BK, Gracz LM, Fahey MA, Elmaleh D, Meltzer PC, Liang AY, Stopa EG, Babich J, Fischman AJ. Altoprane, a SPECT or PET imaging probe for dopamine neurons: III. Human dopamine transporter in postmortem normal and Parkinson's diseased brain. *Synapse* 1998;**29**(2):116-27.
119. Du L, Faludi G, Palkovits M, Demeter E, Bakish D, Lapierre YD, Sotonyi P, Hrdina PD. Frequency of long allele in serotonin transporter gene is increased in depressed suicide victims. *Biol Psychiatry* 1999;**46**(2):196-201.
120. Halldin C, Erixon-Lindroth N, Pauli S, Chou YH, Okubo Y, Karlsson P, Lundkvist C, Olsson H, Guilloteau D, Emond P, Farde L. [¹¹C]PE2I: a highly selective radioligand for PET examination of the dopamine transporter in monkey and human brain. *Eur J Nucl Med Mol Imaging* 2003;**30**(9):1220-30.
121. Wilson A, Ginovart N, Hussey D, Meyer J, Houle S. In vitro and in vivo characterisation of [¹¹C]DASB: a probe for in vivo measurement of the serotonin transporter by positron emission tomography. *Nucl Med Biol* 2002;**29**:509-515.
122. Bracha HS, Garcia-Rill E, Mrak RE, Skinner R. Postmortem locus coeruleus neuron count in three American veterans with probable or possible war-related PTSD. *J Neuropsychiatry Clin Neurosci* 2005;**17**(4):503-9.
123. Kanegawa N, Kiyono Y, Kimura H, Sugita T, Kajiyama S, Kawashima H, Ueda M, Kuge Y, Saji H. Synthesis and evaluation of radioiodinated (S,S)-2-(α -(2-iodophenoxy)benzyl)morpholine for imaging brain norepinephrine transporter. *Eur J Nucl Med Mol Imaging* 2006.

ACKNOWLEDGMENTS

I would like to thank all the people who have helped me during the last five years to complete this thesis work. I would especially like to thank:

My supervisor, Prof. Christer Halldin, for accepting me as a Ph.D. student, for his guidance, support, ideas and for demonstrating an energy and drive without comparison.

My co-supervisor, Prof. Victor W. Pike, for welcoming me to his lab at NIMH, for his guidance, constructive criticism and valuable comments during this thesis work.

Prof. Lars Farde, for help with analysing results and correction of manuscripts.

Arsalan Amir, David Card, Kerstin Larsson and Phong Truong for friendship and excellent technical assistance.

All present and former members of the chemistry group at Karolinska Institutet: Jan Andersson, Dr. Anu Airaksinen, Sean Donohue, Ithamar Brinkmann, Dr. Evgeny Shchukin, Guennadi Jogolev, Dr. Raisa Krasikova, Sangram Nag, Carsten Steiger, Jari Tarkiainen and Sjoerd Finnema for making everyday business a lot easier.

All present and former members of the PET imaging group at Karolinska Institutet: Associate prof. Anna-Lena Nordström, Dr. Bengt Andrée, Jacqueline Borg, Dr. Simon Červenka, Dr. Mirjam Talvik, Nina Erixon-Lindroth, Dr. Johan Lundberg, Kjerstin Lind, Dr. Hans Olsson, Dr. Aurelija Jucaite, Dr. Per Karlsson, Nils Sjöholm, Dr. Stefan Pauli, Dr. Andrea Varrone, Dr. Hristina Jovanovic, Ulla-Kajsa Pehrson and Karin Zahir. In particular Dr. Judit Sóvágó, Julio Gabriel, associate Prof. Balázs Gulyás and Nicholas Seneca for helping out with monkey PET experiments.

Dr. Håkan Hall, Prof. Robert B. Innis, Dr. Jie-Hsan Liow, Dr. Sami S. Zoghbi, Dr. Klaus P. Bøgesø, Dr. P. David Mozley, Dr. David R. Dobson, Dr. Magnus W. Walter and Dr. Peter Gallagher for fruitful collaboration.

The members of the PET chemistry group at NIMH: Dr. Fabrice Simeon, Dr. Julie McCarron, Dr. John Musachio, Jessica Cuevas, Dr. Frederick Chin, Dr. Lisheng Cai, Dr. Umesha Shetty, Cheryl Morse, Dr. Neva Lazarova, Dr. ShuiYu Liu, Kun Park and Jay Shah for making my visit to Bethesda enjoyable.

Henrik Lundqvist, for making a crucial stick-hand save with 25 seconds remaining of the Olympic ice hockey final against Finland.

The people sharing the labs in the basement corridor: Barbro Berthelsson, Alexandra Tylec, Dr. Katarina Varnäs, Monika Horvath, Dr. Katarina Drakenberg, Dr. Pernilla Fagergren, Dr. Xinyu Wang, Hanna Östlund and Maria Stridh for being cheerful and positive.

The present and former members of the Karolinska Pharmacy PET group: Prof. Sharon Stone-Elander, Dr. Jan-Olov Thorell, Dr. Anna Fredriksson, Erik Samen, Erik Engström and Vahid Jalouli for good co-operation in the radiochemistry lab.

My parents Björn and Christina, my sister Therése and my brother Mikael, for being there when I need them.

The Karolinska Institutet and the National Institutes of Health for financial support.